Key Synthetic Analogs of Bleomycin A_2 That Directly Address the Effect and Role of the Disaccharide: Demannosylbleomycin A_2 and α-D-Mannopyranosyldeglycobleomycin A_2

Dale L. Boger,* Shuji Teramoto, and Jiacheng Zhou

Contribution from the Department of Chemistry, The Scripps Research Institute, 10666 North Torrey Pines Road, La Jolla, California 92037

Received January 30, 1995[⊗]

Abstract: Two key synthetic analogs of bleomycin A_2 (**1**) are described. The synthesis and evaluation of demannosylbleomycin A_2 (**3**) lacking the terminal 2-*O*-(3-*O*-carbamoyl)-α-D-mannopyranoside including the putative carbamoyl sixth metal ligand and the monosaccharide **4** in which an α-D-mannopyranose has been substituted for the authentic α-L-gulopyranose with the inversion of the single C5 center of the monosaccharide are detailed. Both agents were prepared through diastereoselective *O*-glycosidation of N^{α}-CBZ-N^{π}-trityl-β-hydroxy-L-histidine methyl ester (**11**) with the diphenyl phosphate of 3,4,6-tri-*O*-acetyl-2-*O*-methyl-β-L-gulopyranose (**10**) and 2,3,4,6-tetra-*O*-acetyl-α-D-mannopyranose (**24**), respectively, followed by sequential tetrapeptide S and pyrimidoblamic acid couplings. The former proceeded with clean inversion of the glycosyl C1 stereochemistry to provide **12** (≥20:1 α:β, 72%) while the latter proceeded with net retention of the glycosyl C1 stereochemistry to provide **26.** Both the low reactivity of the glycosyl acceptor **11** which favors formation of the more stable α-anomer and mechanistic features characteristic of a glycosyl phosphate donor which favor reaction with inversion of the stereochemistry at the reacting anomeric center account for the clean generation of **12** while the mannosylpyranose C2 acetate neighboring group participation in the glycosidation reaction of **24** accounts for the clean generation of **26.** The observation that the DNA cleavage efficiency, selectivity (5′-GC, 5′-GT > 5′-GA), and the double strand versus single strand DNA cleavage ratio of demannosylbleomycin A_2 (**3**) are similar or nearly indistinguishable from bleomycin A_2 (**1**) indicate that the terminal 2-*O*-(3-*O*-carbamoyl)-α-D-mannopyranoside inclusive of the carbamoyl group may have little impact on the DNA cleavage capabilities of the natural agent. In contrast, the substantially diminished DNA cleavage efficiency and ratio of double strand to single strand cleavage events of **4** relative to bleomycin A_2 (**1**), demannosylbleomycin A_2 (**3**), or even deglycobleomycin A_2 (**2**) indicate that the first carbohydrate of the disaccharide may greatly influence the DNA cleavage capabilities of the natural agent. Importantly, the studies indicate that it is the α-L-gulopyranoside segment, not the α-D-mannopyranoside segment inclusive of the carbamoyl group, of the disaccharide that permits the full potentiation of the DNA cleavage properties of bleomycin A_2.

Bleomycin A_2 (**1**), the major constituent of the clinical antitumor agent blenoxane, is thought to derive its therapeutic effects from the ability to mediate the catalytic oxidative cleavage of duplex DNA[1−15] or RNA[16−19] by a process that is metal ion and oxygen dependent. Consequently, bleomycin A_2,[20] its naturally occurring congeners,[21] its degradation products,[22−24] and semisynthetic derivatives[25] as well as a select set of synthetic analogs[2,26−30] have been the subject of extensive and continued examination in efforts to define the fundamental functional roles of the individual subunits.

⊗ Abstract published in *Advance ACS Abstracts,* July 1, 1995.

(1) Natrajan, A.; Hecht, S. M. In *Molecular Aspects of Anticancer Drug-DNA Interactions*; Neidle, S., Waring, M. J., Eds.; CRC Press: Boca Raton, 1994; Vol. 2, 197. Kane, S. A.; Hecht, S. M. In *Progress in Nucleic Acids Research and Molecular Biology*; Cohn, W. E.; Moldave, K., Eds.; Academic Press: San Diego, 1994; Vol. 49, p 313.

(2) Ohno, M.; Otsuka, M. In *Recent Progress in the Chemical Synthesis of Antibiotics*; Lukacs, G., Ohno, M., Eds.; Springer-Verlag: New York, 1990; p 387.

(3) Dedon, P. C.; Goldberg, I. H. *Chem. Res. Toxicol.* **1992**, *5*, 311.

(4) Petering, D. H.; Byrnes, R. W.; Antholine, W. E. *Chem.−Biol. Interact.* **1990**, *73*, 133.

(5) Stubbe, J.; Kozarich, J. W. *Chem. Rev.* **1987**, *87*, 1107.

(6) Hecht, S. M. *Acc. Chem. Res.* **1986**, *19*, 383.

(7) Sugiura, Y.; Takita, T.; Umezawa, H. *Metal Ions Biol. Syst.* **1985**, *19*, 81.

(8) Twentyman, P. R. *Pharmacol. Ther.* **1984**, *23*, 417.

(9) Povirk, L. F. In *Molecular Aspects of Anti-Cancer Drug Action*; Neidle, S., Waring, M. J., Eds.; MacMillian: London, 1983.

(10) *Bleomycin: Chemical, Biochemical and Biological Aspects*; Hecht, S. M., Ed.; Springer-Verlag: New York, 1979.

(11) Umezawa, H. In *Bleomycin: Current Status and New Developments*; Carter, S. K., Crooke, S. T., Umezawa, H., Eds.; Academic Press: New York, 1978.

(12) Ishida, R.; Takahashi, T. *Biochem. Biophys. Res. Commun.* **1975**, *66*, 1432.

(13) Sausville, E. A.; Stein, R. W.; Peisach, J.; Horwitz, S. B. *Biochemistry* **1978**, *17*, 2746.

(14) D'Andrea, A. D.; Haseltine, W. A. *Proc. Natl. Acad. Sci. U.S.A.* **1978**, *75*, 3608.

(15) Takeshita, M.; Grollman, A. P.; Ohtsubo, E.; Ohtsubo, H. *Proc. Natl. Acad. Sci. U.S.A.* **1978**, *75*, 5983.

(16) Hecht, S. M. *Bioconjugate Chem.* **1994**, *5*, 513.

(17) Magliozzo, R. S.; Peisach, J.; Cirolo, M. R. *Mol. Pharmacol.* **1989**, *35*, 428.

(18) Carter, B. J.; de Vroom, E.; Long, E. C.; van der Marel, G. A.; van Boom, J. H.; Hecht, S. M. *Proc. Natl. Acad. Sci. U.S.A.* **1990**, *87*, 9373.

(19) Holmes, C. E.; Carter, B. J.; Hecht, S. M. *Biochemistry* **1993**, *32*, 4293.

(20) Takita, T.; Muraoka, Y.; Nakatani, T.; Fujii, A.; Umezawa, Y.; Naganawa, H.; Umezawa, H. *J. Antibiot.* **1978**, *31*, 801.

(21) Umezawa, H. *Pure Appl. Chem.* **1971**, *28*, 665.

(22) Deglycobleomycin A_2: Oppenheimer, N. J.; Chang, C.; Chang, L.-H.; Ehrenfeld, G.; Rodriguez, L. O.; Hecht, S. M. *J. Biol. Chem.* **1982**, *257*, 1606. Sugiura, Y.; Suzuki, T.; Otsuka, M.; Kobayashi, S.; Ohno, M.; Takita, T.; Umezawa, H. *J. Biol. Chem.* **1983**, *258*, 1328. Sugiura, Y.; Kuwahara, J.; Suzuki, T. *FEBS Lett.* **1985**, *182*, 39. Kenani, A.; Lamblin, G.; Henichart, J.-P. *Carbohydr. Res.* **1988**, *177*, 81. Kenani, A.; Bailly, C.; Helbecque, N.; Catteau, J.-P.; Houssin, R.; Bernier, J.-L.; Henichart, J.-P. *Biochem. J.* **1988**, *253*, 497. Boger, D. L.; Menezes, R. F.; Yang, W. *Bioorg. Med. Chem. Lett.* **1992**, *2*, 959.

(23) Decarbamoylbleomycin A_2: Sugiyama, H.; Ehrenfeld, G. M.; Shipley, J. B.; Kilkuskie, R. E.; Chang, L.-H.; Hecht, S. M. *J. Nat. Prod.* **1985**, *48*, 869. Naganawa, H.; Muraoka, Y.; Takita, T.; Umezawa, H. *J. Antibiot.* **1977**, *30*, 388.

0002-7863/95/1517-7344$09.00/0 © 1995 American Chemical Society

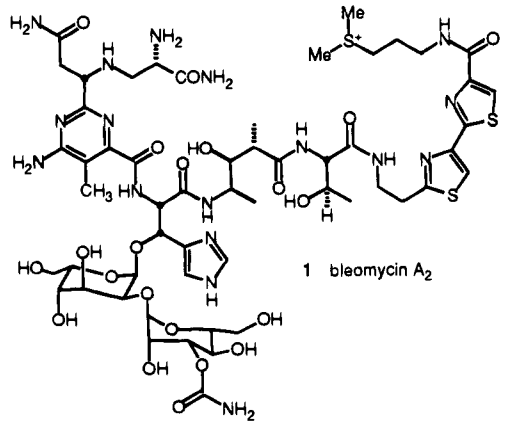

1 bleomycin A_2

Of the bleomycin A_2 subunits, the role of the disaccharide is the most poorly understood. Although it is known not to impact on the characteristic 5′-GC, 5′-GT DNA cleavage selectivity of bleomycin A_2, it is known to make a significant contribution to the DNA cleavage efficiency and the ratio of double strand to single strand DNA cleavage events. For example, the iron complexes of bleomycin A_2 are approximately 2−5 times more effective at cleaving supercoiled ΦX174 DNA (O_2-thiol, Fe(II)) and 6−9 times more effective at cleaving w794/w836 DNA (H_2O_2, Fe(III)) than deglycobleomycin A_2 (**2**) and are more effective in producing double strand versus single strand DNA cleavage (1:6 versus 1:12).[30] Importantly, the DNA binding constants and binding site sizes of bleomycin A_2 and deglycobleomycin A_2 are not distinguishable, indicating that the disaccharide does not contribute to DNA binding affinity and that the enhanced DNA cleavage of properties of **1** do not appear to be due to such features.[30] Moreover, subtle differences in the relative selectivity among the available DNA cleavage sites have been described for bleomycin A_2 (**1**) and deglycobleomycin A_2 (**2**).[22,31] Although there may be many plausible explanations for this, the observation that decarbamoylbleomycin A_2, lacking only the mannose C3-carbamoyl group, behaves like deglycobleomycin A_2 and not bleomycin A_2 has implicated a role for this group in the metal complexation effecting the structure of the coordination complexes.[32,33] It has also been suggested that the bulky disaccharide serves the simple functional role of forming one side of a pocket in conjunction with the C2-acetamido side chain that serves to bind and activate molecular oxygen and ultimately protect the reactive iron oxo or peroxo intermediate of activated bleomycin.[2,22] Consistent with this functional role, simplified metal binding domains incorporated into full analogs of **1** and **2** described in the efforts of Umezawa, Ohno, and co-workers that possess a bulky *tert*-butyl ether replacement for the disaccharide showed substantial enhancements for oxygen activation and catalytic oxidations over the corresponding free alcohol.[26] However, the most effective agent in the series was found to be much less efficient at cleaving DNA than bleomycin A_2, and the cleavage selectivity was not identical with that of **1**.[34] Since bleomycin A_2 is capable of catalytic DNA cleavage with modest turnover (<100), it is conceivable that the disaccharide enhancement is due in part to protective stabilization of the reactive oxidizing agent provided by the pocket.

As a consequence of these issues, we have elected to directly assess the impact and potential role of the disaccharide subunit through the synthesis and evaluation of key structural analogs containing deep-seated disaccharide modifications which are not accessible through modification or degradation of the natural product. Herein, we report the synthesis of **3** and **4** based on our recently disclosed total synthesis of bleomycin A_2.[30] The monosaccharide **3**, demannosylbleomycin A_2, lacks the terminally linked 2-*O*-(3-*O*-carbamoyl)-α-D-mannopyranoside and permits the establishment of its impact on the properties of **1** inclusive of that of the carbamoyl group, a putative sixth ligand for metal complexation. The agent **4** bears a monosaccharide in which the single C5 stereocenter of the linked α-L-gulopyranoside has been inverted to provide a linked α-D-mannopyranoside.

(24) N^{α}-Acetylbleomycin A_2: Oppenheimer, N. J.; Rodriguez, L. O.; Hecht, S. M. *Biochemistry* **1980**, *19*, 4096. N^{α}-Methylbleomycin A_2 and N^{α}-dimethylbleomycin A_2: Fukuoka, T.; Muraoka, Y.; Fujii, A.; Naganawa, H.; Takita, T.; Umezawa, H. *J. Antibiot.* **1980**, *33*, 114. *iso*-Bleomycin A_2: Nakayama, Y.; Kunishima, M.; Omoto, S.; Takita, T.; Umezawa, H. *J. Antibiot.* **1973**, *26*, 400. *epi*-Bleomycin A_2: Muraoka, Y.; Kobayashi, H.; Fujii, A.; Kunishima, M.; Fujii, T.; Nakayama, Y.; Takita, T.; Umezawa, H. *J. Antibiot.* **1976**, *29*, 853. Shipley, J. B.; Hecht, S. M. *Chem. Res. Toxicol.* **1988**, *1*, 25. Deamidobleomycin A_2: Umezawa, H.; Hori, S.; Sawa, T.; Yoshioka, T.; Takeuchi, T. *J. Antibiot.* **1974**, *27*, 419. Deamidobleomycin A_2 and depyruvamidobleomycin A_2: Sugiura, Y. *J. Am. Chem. Soc.* **1980**, *102*, 5208. PEMH and *iso*-bithiazole bleomycin A_2: Morii, T.; Matsuura, T.; Saito, I.; Suzuki, T.; Kuwahara, J.; Sugiura, Y. *J. Am. Chem. Soc.* **1986**, *108*, 7089. Morii, T.; Saito, I.; Matsuura, T.; Kuwahara, J.; Sugiura, Y. *J. Am. Chem. Soc.* **1987**, *109*, 938.

(25) Umezawa, H.; Takita, T.; Saito, S.; Muraoka, Y.; Takahashi, K.; Ekimoto, H.; Minamide, S.; Nishikawa, K.; Fukuoka, T.; Nakatani, T.; Fujii, A.; Matsuda, A. In *Bleomycin Chemotherapy*; Sikic, B. I., Rozenweig, M., Carter, S. K., Eds.; Academic Press: Orlando, 1985; p 289. Takita, T.; Maeda, K. *J. Heterocycl. Chem.* **1980**, *17*, 1799. Vloon, W. J.; Kruk, C.; Pandit, U. K.; Hofs, H. P.; McVie, J. G. *J. Med. Chem.* **1987**, *30*, 20.

(26) Kittaka, A.; Sugano, Y.; Otsuka, M.; Ohno, M. *Tetrahedron* **1988**, *44*, 2811, 2821. Owa, T.; Haupt, A.; Otsuka, M.; Kobayashi, S.; Tomioka, N.; Itai, A.; Ohno, M.; Shiraki, T.; Uesugi, M.; Sugiura, Y.; Maeda, K. *Tetrahedron* **1992**, *48*, 1193. Otsuka, M.; Masuda, T.; Haupt, A.; Ohno, M.; Shiraki, T.; Sugiura, Y.; Maeda, K. *J. Am. Chem. Soc.* **1990**, *112*, 838. Otsuka, M.; Kittaka, A.; Ohno, M.; Suzuki, T.; Kuwahara, J.; Sugiura, Y.; Umezawa, H. *Tetrahedron Lett.* **1986**, *27*, 3639. Total synthesis of bleomycin A_2: Takita, T.; Umezawa, Y.; Saito, S.; Morishima, H.; Naganawa, H.; Umezawa, H.; Tsuchiya, T.; Miyake, T.; Kageyama, S.; Umezawa, S.; Muraoka, Y.; Suzuki, M.; Otsuka, M.; Narita, M.; Kobayasi, S.; Ohno, M. *Tetrahedon Lett.* **1982**, *23*, 521. Saito, S.; Umezawa, Y.; Yoshioka, T.; Takita, T.; Umezawa, H.; Muraoka, Y. *J. Antibiot.* **1983**, *36*, 92.

(27) Kilkuskie, R. E.; Suguna, H.; Yellin, B.; Murugesan, N.; Hecht, S. M. *J. Am. Chem. Soc.* **1985**, *107*, 260. Shipley, J. B.; Hecht, S. M. *Chem. Res. Toxicol.* **1988**, *1*, 25. Carter, B. J.; Murty, V. S.; Reddy, K. S.; Wang, S.-N.; Hecht, S. M. *J. Biol. Chem.* **1990**, *265*, 4193. Hamamichi, N.; Natrajan, A.; Hecht, S. M. *J. Am. Chem. Soc.* **1992**, *114*, 6278. Kane, S. A.; Natrajan, A.; Hecht, S. M. *J. Biol. Chem.* **1994**, *269*, 10899. Quada, J. C.; Levy, M. J.; Hecht, S. M. *J. Am. Chem. Soc.* **1993**, *115*, 12171. Total synthesis of bleomycin A_2: Aoyagi, Y.; Katano, K.; Suguna, H.; Primeau, J.; Chang, L.-H.; Hecht, S. M. *J. Am. Chem. Soc.* **1982**, *104*, 5537.

(28) Kenani, A.; Lohez, M.; Houssin, R.; Helbecque, N.; Bernier, J. L.; Lemay, P.; Henichart, J. P. *Anti-Cancer Drug Design* **1987**, *2*, 47. Kenani, A.; Bailly, C.; Helbecque, N.; Houssin, R.; Bernier, J.-L.; Henichart, J.-P. *Eur. J. Med. Chem.* **1989**, *24*, 371.

(29) Boger, D. L.; Honda, T.; Menezes, R. F.; Colletti, S. L.; Dang, Q .; Yang, W. *J. Am. Chem. Soc.* **1994**, *116*, 82. Boger, D. L.; Yang, W. *Bioorg. Med. Chem. Lett.* **1992**, *2*, 1649. Boger, D. L.; Dang, Q. *J. Org. Chem.* **1992**, *57*, 1631.

(30) Boger, D. L.; Teramoto, S.; Honda, T.; Zhou, J. *J. Am. Chem. Soc.* **1995**, *117*, 7338 (preceding paper in this issue). Boger, D. L.; Colletti, S. L.; Honda, T.; Menezes, R. F. *J. Am. Chem. Soc.* **1994**, *116*, 5607. Boger, D. L.; Honda, T.; Dang, Q. *J. Am. Chem. Soc.* **1994**, *116*, 5619. Boger, D. L.; Honda, T.; Menezes, R. F.; Colletti, S. L. *J. Am. Chem. Soc.* **1994**, *116*, 5631. Boger, D. L.; Honda, T. *J. Am. Chem. Soc.* **1994**, *116*, 5647. Boger, D. L.; Menezes, R. F.; Honda, T. *Angew. Chem., Int. Ed. Engl.* **1993**, *32*, 273. Boger, D. L.; Menezes, R. F.; Dang, Q.; Yang, W. *Bioorg. Med. Chem. Lett.* **1992**, *2*, 261. Boger. D. L.; Menezes, R. F.; Dang, Q. *J. Org. Chem.* **1992**, *57*, 4333. Boger, D. L.; Menezes, R. F. *J. Org. Chem.* **1992**, *57*, 4331.

(31) Shipley, J. B.; Hecht, S. M. *Chem. Res. Toxicol.* **1988**, *1*, 25.

(32) Takita, T.; Muraoka, Y.; Nakatani, T.; Fujii, A.; Iitaka, Y.; Umezawa, H. *J. Antibiot.* **1978**, *31*, 1073.

(33) Oppenheimer, N. J.; Rodriguez, L. O.; Hecht, S. M. *Biochemistry* **1979**, *18*, 3439. Oppenheimer, N. J.; Rodriguez, L. O.; Hecht, S. M. *Proc. Natl. Acad. Sci. U.S.A.* **1979**, *76*, 5616. Sugiura, Y.; Ishizu, K. *J. Inorg. Biochem.* **1979**, *11*, 171. Oppenheimer, N. J.; Chang, C.; Chang, L.-H.; Ehrenfeld, G.; Rodriguez, L. O.; Hecht, S. M. *J. Biol. Chem.* **1982**, *257*, 1606.

(34) Ohno, M.; Otsuka, M.; Kittaka, A.; Sugano, Y.; Sugiura, Y.; Suzuki, T.; Kuwahara, J.; Umezawa, K.; Umezawa, H. *Int. J. Exp. Clin. Chem.* **1988**, *1*, 12.

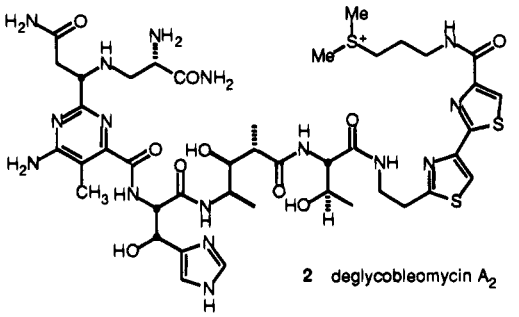

2 deglycobleomycin A_2

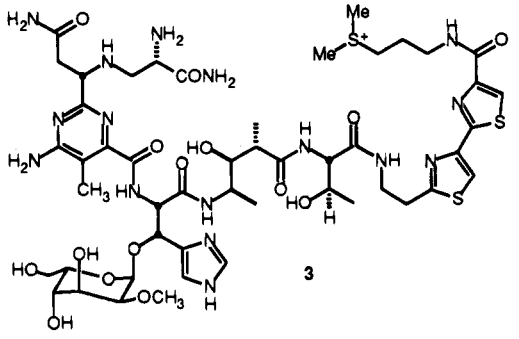

3

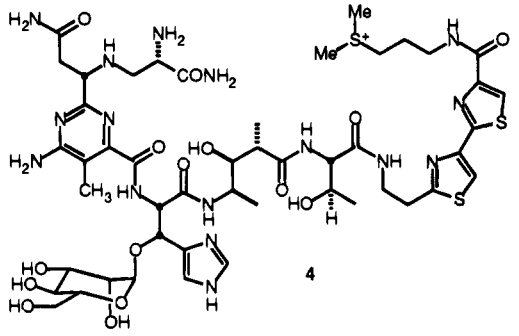

4

The observation that the DNA cleavage efficiency, selectivity, and double strand versus single strand cleavage ratio for **3** are similar or nearly indistinguishable from that of bleomycin A_2 indicates that the terminal 2-*O*-(3-*O*-carbamoyl)-α-D-mannopyranose inclusive of the carbamoyl group has little impact on the DNA cleavage capabilities of the agents. In contrast, the substantially diminished properties of **4**, in which a single stereocenter of **3** is inverted, relative to those of both bleomycin A_2 and deglycobleomycin A_2 indicate that the first carbohydrate of the disaccharide may greatly influence the DNA cleavage capabilities of the agent. The potential origin of these effects is discussed.

Synthesis of Demannosylbleomycin A_2 (3). In efforts to ensure that the comparisons of **1** with a monosaccharide derivative of bleomycin A_2 would represent a direct assessment of the impact of the terminal sugar and not be influenced by the introduction of a free alcohol at the α-L-gulose C2 position, we elected to introduce 2-*O*-methyl-α-L-gulopyranose as the monosaccharide in which a methyl ether caps the C2-hydroxy group involved in the disaccharide glycosyl linkage. The synthesis of the requisite 2-*O*-methyl-L-gulose in a suitably protected form is summarized in Scheme 1. Notably, the starting benzyl 3,4,6-tri-*O*-benzyl-β-L-gulopyranoside (**5**) was prepared from D-mannose with implementation of a regioselective equatorial C3 alcohol alkylation of a 2,3-*O*-dibutylstannylene derivative for differentiation and selective functionalization of the C2 and C3 alcohols followed by a tactically simple D-mannose to L-gulose interconversion by inversion of the C5 stereochemistry as described in our recent total synthesis of bleomycin A_2.[30]

Scheme 1

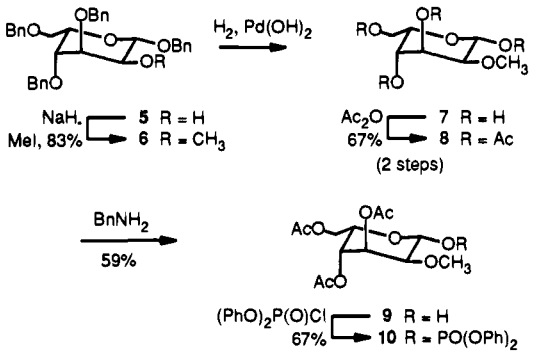

Scheme 2

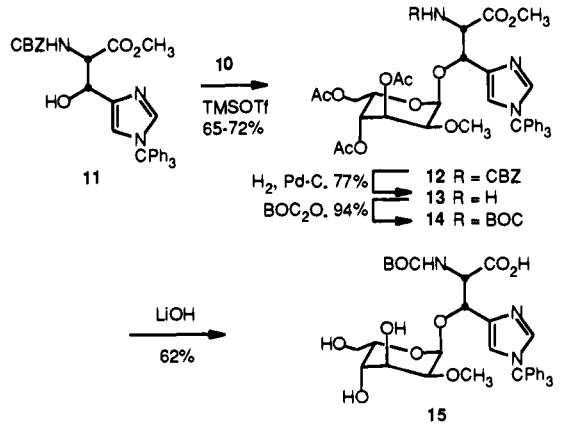

Methylation of **5** which served to cap the L-gulose C2 alcohol followed by exhaustive debenzylation (H_2, 20% $Pd(OH)_2$–C, CH_3OH, 25 °C, 6 h) of **6**, $[\alpha]^{25}_D$ +36.4 (*c* 1.8, $CHCl_3$), and immediate acylation of **7** (12 equiv of Ac_2O, py, 25 °C, 24 h, 67%) provided 1,3,4,6-tetra-*O*-acetyl-2-*O*-methyl-β-L-gulopyranose (**8**, $[\alpha]^{25}_D$ +34 (*c* 0.5, CH_3OH)). Activation of **8** as its β-glycosyl diphenyl phosphate[35] was accomplished by sequential treatment with benzylamine (2.5 equiv, THF, 25 °C, 6 h) for selective deprotection of the glycosyl acetate followed by $(PhO)_2P(O)Cl$ (1.2 equiv, THF, −78 °C, 15 min, 67%) to provide **10**, $[\alpha]^{25}_D$ −15 (*c* 0.5, $CHCl_3$), as a glycosyl donor for coupling with a suitably protected β-hydroxy-L-histidine derivative. Through this sequence, the β-stereochemistry of the L-gulopyranoside anomeric center was maintained and confirmed through observation of diagnostic C1-H/C2-H coupling constants characteristic of an axial C1-H coupled to an adjacent axial C2-H at δ 4.89 (J = 8.0 Hz for **6** C1-H), δ 5.87 (J = 8.3 Hz for **8** C1-H), δ 5.01 (J = 7.9 Hz for **9** C1-H), and δ 5.61 (J = 7.8 Hz for **10** C1-H).

Key to the successful incorporation of **10** into **3** was the method used for the *O*-glycosidation reaction with a suitably protected β-hydroxy-L-histidine derivative and the order of the assemblage of the subunits. The nontrivial selection of the appropriate protecting groups and the nonobvious optimal order of couplings followed those implemented in our successful total synthesis of bleomycin A_2[30] and further benefit from our study of the key *O*-glycosidation reaction in which the use of a β-(diphenyl phosphate) glycosyl donor proved to be unusually successful. Treatment of N^{α}-CBZ-N^{π}-trityl-β-hydroxy-L-histidine methyl ester (**11**)[30] with **10** (2 equiv of TMSOTf, 2:1 Et_2O–CH_2Cl_2, −16 °C, 30 min, 65–72%) provided **12**, $[\alpha]^{25}_D$ −44 (*c* 1.0, CH_3OH), in excellent conversions (Scheme 2). The *O*-glycosidation reaction proceeded to provide the desired

(35) Hashimoto, S.; Honda, T.; Ikegami, S. *J. Chem. Soc., Chem. Commun.* **1989**, 685.

α-anomer (≥20:1). In fact, the undesired β-anomer was not detected and only trace amounts of additional material containing the structural elements of both **10** and **11** were isolated. As such the diastereoselectivity of the glycosidation reaction was estimated to be better than 20:1 and may in fact be higher. Confirmation that the *O*-glycosidation reaction provided the α-anomer with clean inversion of the monosaccharide C1 stereochemistry was derived from the ^{1}H NMR on **12**−**14** with observation of the C1 anomeric proton at δ 5.13 (**13**) and 5.09 (**14**) with a distinguishable coupling constant characteristic (d, J = 3.8 Hz) of an equatorial proton coupled to the adjacent axial C2-H at δ 3.51 (**12**), 3.49 (**13**), and 3.53 (**14**) which also exhibits a set of distinguishable diagnostic coupling constants with the two adjacent C1 and C3 equatorial hydrogens (dd, J = 3.8, 3.8 Hz). The unusually high diastereoselectivity of this glycosidation reaction is noteworthy and may be a consequence of at least two contributing factors. Both the low reactivity of the glycosyl acceptor, which tends to favor formation of the more stable α-anomer, and mechanistic features characteristic of a glycosyl phosphate donor favor reaction with inversion of the stereochemistry at the reacting anomeric center. Selective CBZ deprotection of **12** (0.5 wt equiv of 10% Pd−C, H_2, CH_3OH, 25 °C, 40 min, 77%) proceeded surprisingly uneventfully to provide **13**, $[\alpha]^{25}_D$ −52 (*c* 0.8, CH_3OH), without evidence of competing deprotection of the trityl group. Subsequent BOC protection of the free amine of **13** (3 equiv of BOC_2O, 6 equiv of $NaHCO_3$, 3:1 THF−H_2O, 25 °C, 3 h, 94%) followed by exhaustive ester hydrolysis (6 equiv of LiOH, CH_3OH, 4 °C, 2.5 h, 62%) of **14**, $[\alpha]^{25}_D$ −46 (*c* 1.0, CH_3OH), provided **15**, $[\alpha]^{25}_D$ −12 (*c* 0.5, CH_3OH), suitably protected for sequential couplings with tetrapeptide S and N^{α}-BOC-pyrimidoblamic acid. Attempts to conduct the hydrolysis of **14** with NaOH (12 equiv, 1 N aqueous NaOH, CH_3OH, 4 °C, 20 h) or when conducted for longer reaction periods led to competitive base-catalyzed β-elimination of the monosaccharide.

Coupling of **15** with the free amine of tetrapeptide S (**16**,[30] 1.1 equiv, 3 equiv of DCC, 1.8 equiv of HOBt, 3.5 equiv of $NaHCO_3$, DMF, 25 °C, 22 h, 76%) provided **17**, $[\alpha]^{25}_D$ −2.9 (*c* 0.25, CH_3OH), in excellent yield (Scheme 3). Notably, the coupling was conducted without deliberate protection of the free hydroxyl groups and with the tetrapeptide S terminal sulfonium salt installed in the substrate. Selective N^{α}-BOC deprotection of **17** under the conditions defined by Sieber and Riniker[36] (1 N HCl in 90% aqueous HOAc, 25 °C, 5 min, 89%) provided **18**, $[\alpha]^{25}_D$ −11 (*c* 0.15, CH_3OH), derived from removal of the BOC protecting group without competitive deglycosidation or removal of the trityl protecting group. Subsequent coupling of **18** with N^{α}-BOC-pyrimidoblamic acid (**19**,[30] 1.0 equiv, 3 equiv of DCC, 1.5 equiv of HOBt, DMF, 25 °C, 24 h, 73%) provided **20**, $[\alpha]^{25}_D$ −2 (*c* 0.1, CH_3OH), and was conducted without protection of the free hydroxyl groups and with the terminal sulfonium salt intact. Final acid-catalyzed deprotection of **20** (20% CF_3CO_2H−CH_2Cl_2, 4 °C, 2.5 h, 77%) provided **3**, $[\alpha]^{25}_D$ −1.7 (*c* 0.1, CH_3OH).

Synthesis of 4. In an effort to distinguish the relative importance of the first carbohydrate of the disaccharide, the agent **4** in which the α-L-gulose was replaced with α-D-mannose was targeted for synthesis and evaluation. With this replacement, the single C5 stereochemistry of the monosaccharide L-α-gulose of **3** was inverted. The synthesis of **4** is summarized in Schemes 4 and 5. The α-D-mannopyranose glycosyl donor was prepared as shown in Scheme 4 from methyl α-D-mannopyranoside **21** by sequential peracetylation (cat. H_2SO_4, Ac_2O, 25 °C, 12 h, 97%), selective hydrolysis of the C1 anomeric acetate

Scheme 3

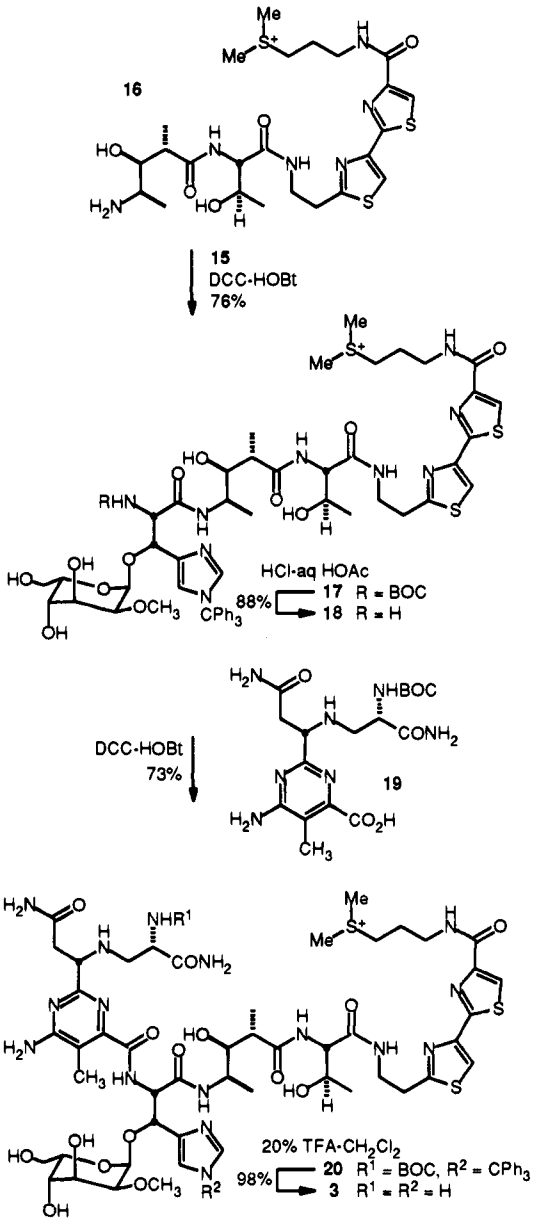

(2.5 equiv of $BnNH_2$, THF, 25 °C, 3 h, 73%),[35] and subsequent activation of the anomeric center through conversion of **23**[37] to the diphenyl phosphate **24** (1.2 equiv of $ClP(O)(OPh)_2$, THF, −78 °C, 25 min, 64%) and the trichloroacetimidate **25** (0.7 equiv of NaH, Cl_3CCN, CH_2Cl_2, 25 °C, 15 min, 69%).[38] In contrast to **25** which failed to provide **26** upon treatment with BF_3•OEt_2, treatment of N^{α}-CBZ-N^{π}-trityl-β-hydroxy-L-histidine methyl ester (**11**)[30] with **24** (1.4 equiv of TMSOTf, 2:1 Et_2O−CH_2Cl_2, 0 °C, 2 h, 32%) provided **26**, $[\alpha]^{21}_D$ +38 (*c* 0.5, $CHCl_3$). Similarly, *O*-glycosidation of **11** with **25** catalyzed by treatment with TMSOTf (1.5 equiv, Et_2O−CH_2Cl_2 2:1, 0 °C, 45 min) provided **26** but in lower conversions. In both instances, only a single stereoisomer of the *O*-glycosidation product was detected. These initial studies provided sufficient amounts of **26** for completion of the preparation of **4** and thus was carried forward without further optimization. Clean generation of the α-linked stereochemistry with net retention of the reacting anomeric α-configuration was observed, may be attributed to

(36) Sieber, P.; Riniker, B. *Tetrahedron Lett.* **1987**, *28*, 6031.

(37) $[\alpha]^{22}_D$ +22.8 (*c* 1.0, $CHCl_3$), lit $[\alpha]^{22}_D$ +23.1 (*c* 4.6, $CHCl_3$); Bonner, W. A. *J. Am. Chem. Soc.* **1958**, *80*, 3372.

(38) Schmidt, R. R.; Grundler, G. *Synthesis* **1981**, 885.

Scheme 4

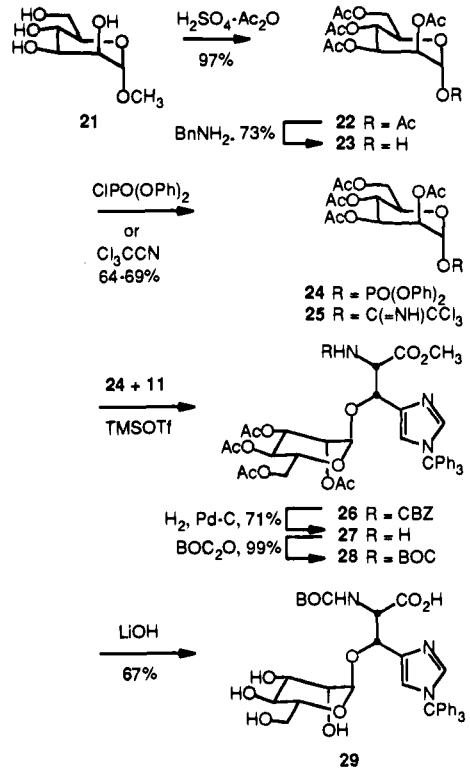

the neighboring group participation by the mannopyranosyl C2 acetate, and was confirmed by observation of diagnostic and large C1/C1-H coupling constant (J = 171 Hz) characteristic of an equatorial hydrogen at the anomeric center. Clean and selective CBZ deprotection of **26** was accomplished by catalytic hydrogenolysis (0.5 wt equiv of 10% Pd–C, H_2, CH_3OH, 45 min, 71%) without competitive trityl deprotection and provided **27**, $[\alpha]^{25}_D$ +53 (c 0.5, CH_3OH). Reprotection of the free amine of **27** (3.6 equiv of BOC_2O, 6 equiv of $NaHCO_3$, 3:1 THF–H_2O, 25 °C, 1.5 h, 99%) followed by exhaustive ester hydrolysis of **28**, $[\alpha]^{22}_D$ +42 (c 0.7, $CHCl_3$), (7 equiv of LiOH, 2:1 CH_3OH–H_2O, 4 °C, 3 h, 67%) provided **29**, $[\alpha]^{22}_D$ +42 (c 0.7, CH_3OH).

Coupling of **29** with the free amine of tetrapeptide S (**16**,[30] 2 equiv of DCC, 1.3 equiv of HOBt, 10 h, 25 °C, 64%) provided **30**, $[\alpha]^{21}_D$ +54 (c 0.3, CH_3OH), in excellent yield (Scheme 5). Selective N^{α}-BOC deprotection (1 N HCl in 90% aqueous HOAc, 25 °C, 5 min, 67%, 82% based on recovered **30**)[36] followed by coupling of **31**, $[\alpha]^{21}_D$ +46 (c 0.2, CH_3OH), with N^{α}-BOC-pyrimidoblamic acid (**19**,[30] 2 equiv of DCC, 1.3 equiv of HOBt, 10 h, 25 °C, 81%) provided **32**, $[\alpha]^{22}_D$ +39 (c 0.13, CH_3OH). Final acid-catalyzed deprotection of **32** (20% CF_3CO_2H–CH_2Cl_2, 4 °C, 2.5 h, 94%) provided **4**, $[\alpha]^{21}_D$ +41 (c 0.1, CH_3OH).

DNA Cleavage Properties of 3 and 4. The first study of the relative efficiency of DNA cleavage was conducted with the Fe(II) complexes of **3** and **4** in the presence of O_2 and 2-mercaptoethanol as an appropriate reducing agent. The assessment was made through the examination of the single and double strand cleavage of supercoiled ΦX174 RFI DNA (form I) to produce relaxed (form II) and linear (form III) DNA, respectively. Like Fe(II)–bleomycin A_2 (**1**)[3,5–7,30] and deglycobleomycin A_2 (**2**),[22] the Fe(II) complexes of **3** and **4** produced both single and double strand cleavage of the supercoiled DNA (Table 1). Demannosylbleomycin A_2 (**3**) proved similar and nearly indistinguishable from bleomycin A_2 (**1**) and 2–4 times more effective than deglycobleomycin A_2 (**2**). Consistent in a series of assays, **3** was slightly less efficient than bleomycin A_2 itself (0.5–1 times) and easily assessed as being substantially more effective than deglycobleomycin A_2. In contrast, **4** proved to be substantially less efficient (2–5 times) than bleomycin A_2 and essentially equivalent to deglycobleomycin A_2 (**2**). Consequently, the removal of the terminal carbohydrate from **1** only resulted in a small reduction in the DNA cleavage efficiency and had less impact than anticipated. In contrast,

Scheme 5

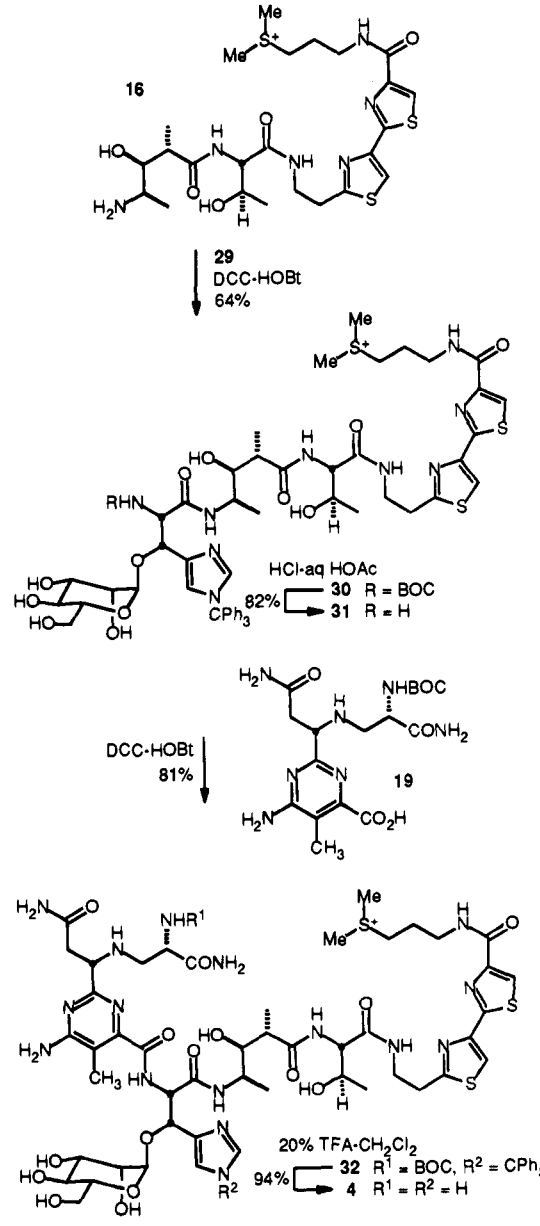

Table 1. Summary of ΦX174 RFI DNA Cleavage Properties: Fe(II) Complexes, O_2 Activation, Mercaptoethanol Initiation

agent	relative efficiency of DNA cleavage[a]	ratio of double to single strand DNA cleavage[b]
bleomycin A_2 (**1**)	2–5	1:6
deglycobleomycin A_2 (**2**)	1.0	1:12
demannosylbleomycin A_2 (**3**)	2–4	1:7
mannosyldeglycobleomycin A_2 (**4**)	1.0	1:20
Fe(II)	0.04	1:98

[a] Relative efficiency of supercoiled ΦX174 DNA cleavage. [b] Ratio of double to single strand cleavage of supercoiled ΦX174 DNA cleavage calculated as $F_{III} = n_2 \exp(-n_2)$, $F_I = \exp[-(n_1 + n_2)]$.

Table 2. Summary of DNA Cleavage Sites of Fe(III)−**3** and Fe(III)−**4** within w794 and w836 DNA

cleavage sites	no. of cleavage sites	total no. of dinucleotide sites	%	cleavage sites	no. of cleavage sites	total no. of dinucleotide sites	%
5′-GC	29	29	100	5′-TT	1	13	8
5′-GT	5	5	100	5′-TA	1	15	7
5′-GA	11	14	79	5′-TC	0	19	0
5′-GG	0	28	0	5′-TG	0	10	0
5′-AT	7	18	39	5′-CT	1	20	5
5′-AC	2	7	28	5′-CC	0	38	0
5′-AA	3	24	13	5′-CA	0	18	0
5′-AG	0	22	0	5′-CG	0	17	0

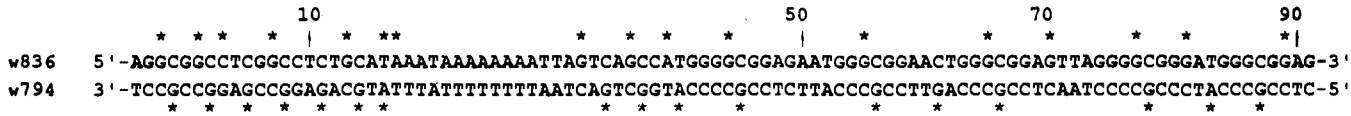

Figure 1. Summary of cleavage sites for the bleomycins with w794 and w836 DNA. The missing terminal regions of the DNA not shown from which some of the data for Table 2 was taken represent the nonoverlapping regions not present on the complementary clones.

the nature of the first carbohydrate had a significant impact, and the simple inversion of one natural stereocenter resulted in the substantial reduction in DNA cleavage efficiency (2−4 times), providing an agent comparable to **2** which lacks the disaccharide altogether. The lack of DNA cleavage by the agents alone in the absence of Fe(II) in control studies is consistent with expectations that the agents are cleaving DNA by a metal-dependent oxidative process in a manner analogous to that of **1** and **2**.

Although both single and double strand DNA lesions result from the radical-mediated oxidative cleavage of DNA by bleomycin A_2, the latter have been considered the more significant biological event.[3] Consequently, the relative extent of double to single strand DNA cleavage was established for **1**−**4** in a study of the kinetics of cleavage to produce linear and circular DNA employing the Fe(II) complexes and supercoiled ΦX174 DNA.[30] Typical results are summarized in Table 1. The reactions show initial fast kinetics in the first 1−10 min, and the subsequent decreasing rate of DNA cleavage may reflect conversion to a less active or inactive agent or metal complex reactivation kinetics. We assumed a Poisson distribution for the formation of single and double strand breaks to calculate the average number of double and single strand cuts per DNA molecule using the Freifelder−Trumbo equation.[39] The data for the first few minutes (1−10 min) could be fitted to a linear equation, and the ratios of double to single strand cuts observed with the Fe(II) complexes of **3** and **4** are summarized in Table 1. A theoretical ratio of approximately 1:100 is required in order for the linear DNA to be the result of the random accumulation of single strand breaks within the 5386 base pair size of ΦX174 DNA, assuming that sequential cleavage on the complementary strands within 15 base pairs is required to permit formation of linear DNA from the hybridized duplex DNA. Experimentally it was determined that Fe(II) alone produced a ratio of 1:98 double strand to single strand breaks under our conditions of assay consistent with the theoretical ratio. Demannosylbleomycin A_2 (**3**, 1:7) proved essentially indistinguishable from bleomycin A_2 (**1**, 1:6), significantly more effective than deglycobleomycin A_2 (**2**, 1:12), and much more effective than **4** (1:20). Thus, while the removal of the terminal carbohydrate of the bleomycin A_2 disaccharide had no effect on the ratio of double to single strand DNA cleavage events, the inversion of a single stereocenter within the first carbohydrate substantially reduced this capability and provided an agent that was less effective than deglycobleomycin A_2 (**2**) which lacks a linked mono- or disaccharide.

(39) Freifelder, D.; Trumbo, B. *Biopolymers* **1969**, *7*, 681.

The selectivity of DNA cleavage and a second assessment of the relative DNA cleavage efficiency were examined within duplex w794 DNA and its complement w836 DNA[40] by monitoring strand cleavage of singly ^{32}P 5′-end-labeled double-stranded DNA[41] after exposure to the Fe(III) complexes of the agents following activation with H_2O_2[42] in 10 mM phosphate buffer (pH 7.0). Thus, incubation of the labeled duplex DNA with the agents in the presence of equimolar $FeCl_3$ and H_2O_2 (50 mM) led to DNA cleavage. Removal of the agent by EtOH precipitation of the DNA, resuspension of the treated DNA in aqueous buffer, and high-resolution polyacrylamide gel electrophoresis (PAGE) of the resultant DNA under denaturing conditions adjacent to Sanger sequencing standards permitted the identification of the sites of DNA cleavage. An extensive range of conditions for the DNA cleavage reactions was examined, including reaction temperature and time (0 °C, 10 min to 1 h; 25 °C, 10 min to 1 h; 37 °C, 10−30 min), buffer (10 mM phosphate, pH 5.7 and 7.0; 10 mM phosphate/10 mM KCl, pH 5.7 and 7.0; 2.5 mM phosphate/1.25 mM KCl, pH 5.7 and 7.0). Among the conditions examined, **1**−**4** were found to cleave DNA most effectively when the reactions were conducted at 37 °C for 30 min in 10 mM phosphate/10 mM KCl buffer at pH 7.0.[30]

A statistical treatment of the observed and available dinucleotide DNA cleavage sites detected with the agents **3** and **4** is summarized in Table 2, and the observed sites of DNA cleavage within w794 and w836 DNA are illustrated in Figure 1. The two w794 PAGE shown in Figures 2 and 3 illustrate clearly that little or no distinguishing differences in the sequence selectivity of DNA cleavage were observed between the synthetic monosaccharide analogs **3** and **4** and natural products bleomycin A_2 (**1**) and deglycobleomycin A_2 (**2**). Consistent with prior studies, only subtle differences in the relative selectivity of cleavage at the various dinucleotide sites were detected,[23,31,43,44] and we did not observe differences in the dinucleotide cleavage

(40) Ambrose, C.; Rajadhyaksha, A.; Lowman, H.; Bina, M. *J. Mol. Biol.* **1989**, *209*, 255.

(41) Boger, D. L.; Munk, S. A.; Zarrinmayeh, H.; Ishizaki, T.; Haught, J.; Bina, M. *Tetrahedron* **1991**, *47*, 2661.

(42) Natrajan, A.; Hecht, S. M.; van der Marel, G. A.; van Boom, J. H. *J. Am. Chem. Soc.* **1990**, *112*, 3997. Natrajan, A.; Hecht, S. M.; van der Marel, G. A.; van Boom, J. H. *J. Am. Chem. Soc.* **1990**, *112*, 4532.

(43) Ehrenfeld, G. M.; Shipley, J. B.; Heimbrook, D. C.; Sugiyama, H.; Long, E. C.; van Boom, J.-H.; van der Marel, G. A.; Oppenheimer, N. J.; Hecht, S. M. *Biochemistry* **1987**, *26*, 931.

(44) Sugiyama, H.; Kilkuskie, R. E.; Chang, L.-H.; Ma, L.-T.; Hecht, S. M. *J. Am. Chem. Soc.* **1986**, *108*, 3852. Sugiyama, H.; Xu, C.; Murugesan, N.; Hecht, S. M.; van der Marel, G. A.; van Boom, J. H. *Biochemistry* **1988**, *27*, 58.

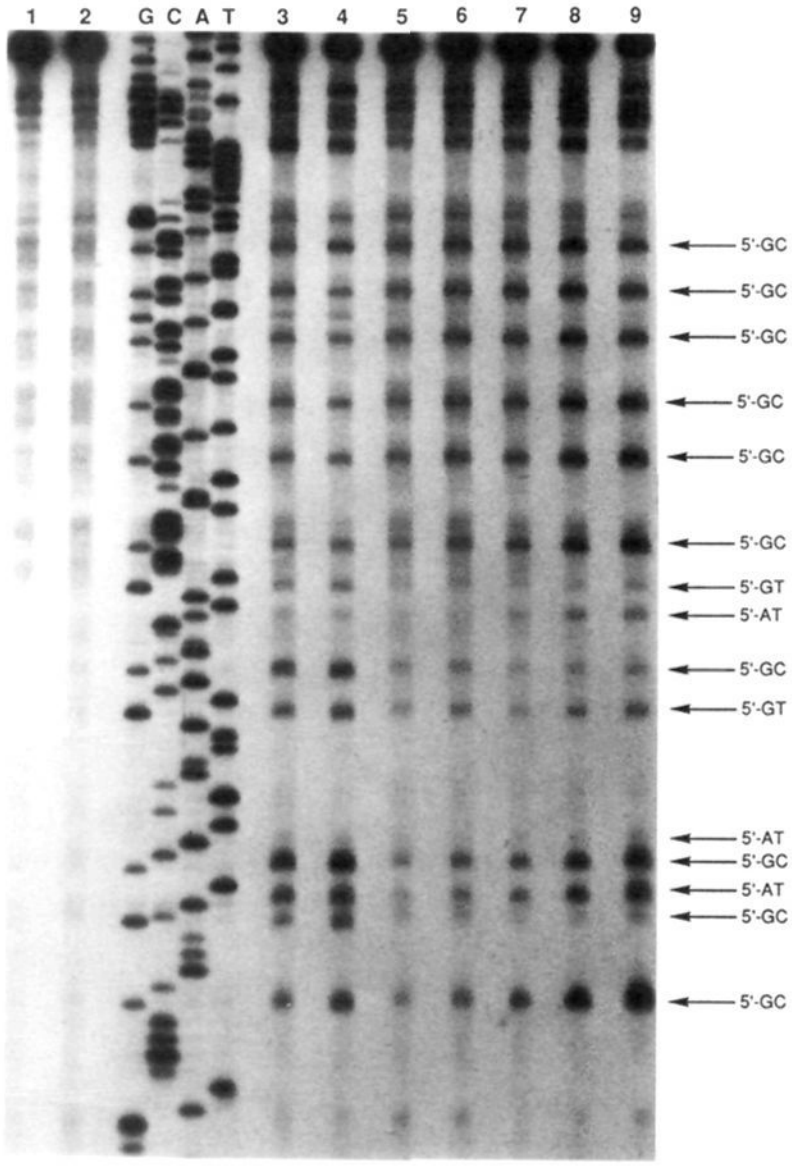

Figure 2. Cleavage of double strand DNA (SV40 DNA fragment, 156 base pairs, nucleotide no. 5239-150, clone w794) in 10 mM phosphate/10 mM KCl buffer, pH 7.0, containing H_2O_2 by Fe(III)−bleomycins. The DNA cleavage reactions were run for 30 min at 37 °C, and electrophoresis was conducted at 1100 V (5.5 h) on a 8% denaturing PAGE and visualized by autoradiography. Lane 1, control DNA; lane 2, 4 μM Fe(III) control; lanes 3 and 4, 0.2 and 0.5 μM Fe(III)−bleomycin A_2 (**1**); lanes 5 and 6, 2.0 and 4.0 μM Fe(III)−deglycobleomycin A_2 (**2**); lanes 7−9, 0.2, 0.5, and 1.0 μM Fe(III)−**3**.

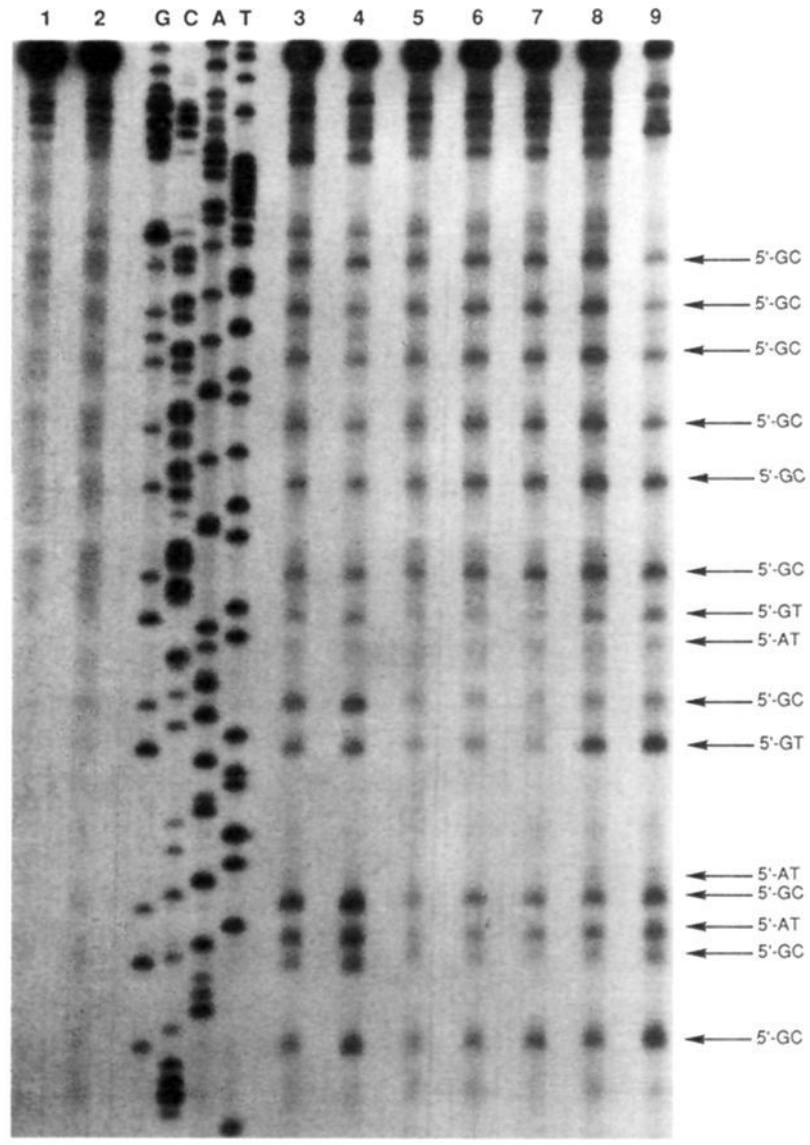

Figure 3. Cleavage of double strand DNA (SV40 DNA fragment, 156 base pairs, nucleotide no. 5239-150, clone w794) in 10 mM phosphate/10 mM KCl buffer, pH 7.0, containing H_2O_2 by Fe(III)−bleomycins. The DNA cleavage reactions were run for 30 min at 37 °C, and electrophoresis was conducted at 1100 V (5.5 h) on a 8% denaturing PAGE and visualized by autoradiography. Lane 1, control DNA; lane 2, 8 μM Fe(III) control; lanes 3 and 4, 0.2 and 0.5 μM Fe(III)−bleomycin A_2 (**1**); lanes 5 and 6, 2.0 and 4.0 μM Fe(III)−deglycobleomycin A_2 (**2**); lanes 7−9, 2.0, 4.0, and 8.0 μM Fe(III)−**4**.

sites that have been occasionally attributed to decarbamoylbleomycin A_2.[31]

Quantitation of the consumption of the labeled DNA representing an accurate measure of the extent of DNA cleavage provided an additional assessment of the relative efficiency of DNA cleavage under a second set of conditions (Fe(III) complex, H_2O_2 activation versus Fe(II) complex, O_2, 2-mercaptoethanol initiation). The results of the quantitative assessment for w794 DNA are summarized in Table 3 and take into account the different concentrations of complex employed in the DNA cleavage reaction. The same order and the same relative quantitative trends in the DNA cleavage efficiency were observed with the w794 DNA protocol that were observed with ΦX174 DNA, although this assay is more sensitive and the absolute magnitudes of the differences are usually expectedly magnified.[30] This, no doubt, reflects the two different procedures employed for agent activation and initiation of DNA cleavage and the conditions of the assay. Although no significant differences in the dinucleotide cleavage selectivity for **1**−**4** were detected, substantial differences in their relative efficiency of DNA cleavage were observed. Little perceptible difference between demannosylbleomycin A_2 (**3**) and bleomycin A_2 (**1**) was observed in this sensitive assay, clearly indicating that the terminal carbohydrate of the disaccharide is contributing little to the DNA cleavage capabilities of the Fe(III) complex of the natural agent. In this assay, Fe(III)−**3** behaved even more similar to Fe(III)−bleomycin A_2 than the Fe(II) complexes examined in the ΦX174 DNA assay. Both **3** (4.5 times) and **1** (4.9−5.2 times) were substantially more effective than deglycobleomycin A_2 (**2**). In contrast, the monosaccharide **4** in which a single stereocenter of **3** is inverted was found to be 8−10 times less effective than **1** and **3** and 1.6 times less efficient than deglycobleomycin A_2 (**2**), which lacks a linked carbohydrate. This clearly indicates that the first carbohydrate of the disaccharide greatly enhances the properties of the natural agent, that the second carbohydrate plays little or no perceptible role, and that the structure of the first linked carbohydrate is very important.

Discussion

As detailed in previous studies,[30] bleomycin A_2 (**1**, $K_B = 1.0 \times 10^5$ M^{-1}, 3.9 base pair binding site size) and deglycobleomycin A_2 (**2**, $K_B = 1.1 \times 10^{-5}$ M^{-1}, 3.8 base pair binding site size) exhibit the same apparent DNA binding affinity, apparent binding site size, and DNA cleavage selectivity. Despite these similarities, they possess substantially different DNA cleavage efficiencies and ratios of double to single strand DNA cleavage events (Tables 1 and 3). As a consequence, the relative comparisons of **1**−**4** permit a direct structural assessment of the origin of the effect and role of the bleomycin A_2 disaccharide subunit. To date most considerations of the role of the bleomycin A_2 disaccharide have focused on the carbamoyl group located on the terminal carbohydrate and its potential role as a

Table 3. Summary of w794 DNA Cleavage Properties: Fe(III) Complexes and H_2O_2 Activation

agent	relative efficiency of DNA cleavage[a]	DNA cleavage selectivity[b]
bleomycin A_2 (**1**)	4.9–5.2	5′-GC, 5′-GT > 5′-GA
deglycobleomycin A_2 (**2**)	1.0	5′-GC, 5′-GT > 5′-GA
demannosylbleomycin A_2 (**3**)	4.5	5′-GC, 5′-GT > 5′-GA
mannosyldeglycobleomycin A_2 (**4**)	0.6	5′-GC, 5′-GT > 5′-GA
Fe(III)	0.006	none

[a] Relative efficiency of 5′-end-labeled w794 DNA cleavage. The different concentrations of complex employed in the DNA cleavage reaction were taken into account in the quantitation of the consumption of labeled DNA. [b] 5′-GC, 5′-GT > 5′-GA > 5′-AT > 5′-AC > 5′-AA, 5′-TT, 5′-TA, 5′-CT, see Table 2.

ligand in the metal complexation. In these comparisons, the Fe(II) complexes of decarbomoylbleomycin A_2 (84–97%)[23,43,44] and isobleomycin A_2 (50%)[31,43] have exhibited a DNA cleavage efficiency not dissimilar from that of bleomycin A_2 (100%) itself. In addition, both similarities and subtle distinctions in the DNA dinucleotide cleavage selectivities of deglycobleomycin A_2, decarbamoylbleomycin A_2, isobleomycin A_2, and bleomycin A_2 have been described. Although the strand scission selectivity of decarbamoylbleomycin A_2, isobleomycin A_2,[31] and bleomycin A_2 was often perceived to be essentially the same,[23,43] significant differences between the agents have been detailed[31] including a different strand selectivity within a defined duplex oligonucleotide.[44] This has been attributed to differences in the N-terminus geometry of the metal complexes with implications for a role of the carbamoyl group in determining or altering the coordination geometry.[44] This has naturally placed a potential importance on the role of the terminal 2-*O*-(3-*O*-carbamoyl)-α-D-mannopyranoside. The comparisons of demannosylbleomycin A_2 (**3**) with bleomycin A_2 (**1**) detailed herein indicate that the DNA cleavage efficiency, selectivity, and double versus single strand DNA cleavage events are nearly indistinguishable and that the terminal 2-*O*-(3-*O*-carbamoyl)-α-D-mannopyranoside inclusive of the carbamoyl group has little impact on the DNA cleavage capabilities of the agents. Consequently, its role in the metal complexation, oxygen activation, and DNA cleavage is clearly subtle.

In sharp contrast, the comparisons of **1**–**3** with **4** in which an α-D-mannopyranoside has been substituted for the authentic α-L-gulopyranoside with inversion of the single C5 stereocenter of the monosaccharide indicate that the structure of the first carbohydrate of the disaccharide is more important. Although **1**–**4** all exhibited essentially the same DNA cleavage selectivity, the agent **4** was substantially less effective than bleomycin A_2 (**1**) and demannosylbleomycin A_2 (**3**) and even less effective than deglycobleomycin A_2 (**2**). It is conceivable that the disaccharide enhancement is simply derived from protective stabilization of the iron oxo reactive intermediate of activated bleomycin A_2 and that the first monosaccharide is sufficient to provide the protective stabilization. However, the observations made with monosaccharide **4** which proved less effective than **2** lacking a linked carbohydrate suggest that the monosaccharide role is more complementary to the action of bleomycin A_2 than simple protective stabilization. It may conceivably contribute to the natural agent adoption of a productive DNA bound conformation that leads to DNA cleavage. Although it is the single C5 stereocenter of the monosaccharides of **3** versus **4** that is inverted, this can be expected to have a pronounced effect on the conformation and orientation of the linked carbohydrate. This is depicted in the structures **3** versus **4** where the C1/C2 stereochemistry is cis in **3** but trans in **4** by virtue of the α-axial anomeric linkage and where each of the C2, C3, and C4 substituents on the monosaccharides can be expected to adopt opposite axial or equatorial positions in the two agents. Thus, the two agents are substantially different, and it is not surprising that **4** exhibits properties distinct and diminished from that of **1** or **3**.[45] Importantly, the comparisons demonstrate that it is the α-L-gulopyranoside segment, not the α-D-mannopyranoside segment, of the disaccharide that permits full potentiation of the DNA cleavage properties of bleomycin A_2.

Experimental Section

Benzyl 3,4,6-Tri-*O*-benzyl-2-*O*-methyl-β-L-gulopyranoside (6). NaH (42 mg, 1.3 mmol) was added to a solution of benzyl 3,4,6-tri-*O*-benzyl-β-L-gulopyranoside (**5**, 0.59 g, 1.09 mmol) in DMF (6 mL) at 25 °C under N_2. The reaction mixture was stirred for 1 h at 25 °C and 20 min at 50 °C. MeI (82 μL, 1.3 μmol) was added at 0 °C, and the resulting solution was stirred for 15 min at 25 °C prior to the addition of additional NaH (42 mg). The resulting solution was stirred for 1 h at 25 °C and 20 min at 50 °C. Additional MeI (82 μL) was added at 0 °C, and the reaction mixture was stirred for 20 min at 25 °C. The reaction mixture was poured into a two-phase solution of EtOAc (50 mL) and H_2O (30 mL). The organic layer was washed with H_2O (30 mL) and saturated aqueous NaCl (30 mL), dried (Na_2SO_4), and concentrated in vacuo. Chromatography (SiO_2, 1.8 × 17 cm, 10% EtOAc–hexane) provided **6** (0.50 g, 0.60 g theoretical, 83%) as a colorless syrup: R_f 0.6 (SiO_2, 20% EtOAc–hexane); $[\alpha]^{25}_D$ +36.4 (*c* 1.8, $CHCl_3$); ^{1}H NMR ($CDCl_3$, 400 MHz) δ 7.18–7.40 (20H, m), 4.94 (1H, d, *J* = 11.9 Hz), 4.89 (1H, d, *J* = 8.0 Hz), 4.70 (1H, d, *J* = 12.2 Hz), 4.62 (1H, d, *J* = 11.9 Hz), 4.40–4.56 (5H, m), 4.11 (1H, ddd, *J* = 1.5, 6.3, 6.6 Hz), 3.87 (1H, dd, *J* = 3.2, 3.5 Hz), 3.65 (1H, dd, *J* = 6.3, 9.8 Hz), 3.60 (1H, dd, *J* = 6.6, 9.8 Hz), 3.50 (1H, dd, *J* = 1.5, 3.5 Hz), 3.47 (3H, s), 3.43 (1H, dd, *J* = 3.2, 8.0 Hz); ^{13}C NMR ($CDCl_3$, 100 MHz) δ 138.3, 138.2, 138.0, 128.3, 128.2, 128.1, 127.9, 127.8, 127.7, 127.6, 127.3, 100.2, 78.7, 74.7, 74.4, 73.4, 73.3, 72.8, 72.0, 70.6, 68.9, 59.4; IR (neat) ν_{max} 3029, 2871, 1453, 1204, 1087, 1027 cm^{-1}; FABHRMS (NBA) *m/e* 687.1696 (M^+ + Cs, $C_{35}H_{38}O_6$ requires 687.1722).

1,3,4,6-Tetra-*O*-acetyl-2-*O*-methyl-β-L-gulopyranose (8). A solution of **6** (0.40 g, 0.72 mmol) in CH_3OH (10 mL) was hydrogenated over 20% $Pd(OH)_2$–C (0.10 g) under an atmosphere of H_2 (1 atm) at 25 °C for 6 h. The reaction mixture was filtered through a Celite pad and concentrated in vacuo. The residue was dissolved in pyridine (5 mL) and treated with Ac_2O (0.81 mL, 8.63 mmol). The reaction mixture was stirred for 24 h at 25 °C before being poured into a two-phase solution of EtOAc (20 mL) and H_2O (20 mL). The organic layer was washed with 10% aqueous HCl (20 mL), H_2O (20 mL), saturated aqueous $NaHCO_3$ (20 mL), H_2O (20 mL), and saturated aqueous NaCl (20 mL). The organic layer was dried (Na_2SO_4) and concentrated in vacuo. Chromatography (SiO_2, 1.4 × 12 cm, 33% EtOAc–hexane) gave **8** (178 mg, 261 mg theoretical, 67%) as a colorless syrup: R_f 0.4 (SiO_2, 50% EtOAc–hexane); $[\alpha]^{25}_D$ +34 (*c* 0.55, CH_3OH); ^{1}H NMR ($CDCl_3$, 400 MHz) δ 5.87 (1H, d, *J* = 8.3 Hz), 5.49 (1H, dd, *J* = 3.6, 3.6 Hz), 5.00 (1H, dd, *J* = 1.5, 3.6 Hz), 4.31 (1H, ddd, *J* = 1.5, 5.8, 7.1 Hz), 4.16 (1H, dd, *J* = 5.8, 11.5 Hz), 4.08 (1H, dd, *J* = 7.1, 11.5 Hz), 3.47 (1H, dd, *J* = 3.6, 8.3 Hz), 3.40 (3H, s), 2.17 (3H, s), 2.15 (3H, s), 2.15 (3H, s), 2.06 (3H, s); ^{13}C NMR ($CDCl_3$, 100 MHz) δ 170.5, 169.3, 169.2, 169.0, 91.5, 75.3, 71.1, 67.7, 66.5, 61.6, 58.5, 21.0, 20.8, 20.7 (2C); IR (neat) ν_{max} 2940, 1759, 1372, 1218, 1114, 1069

(45) It is also possible that the distinguishing features of **3** and **4** may be attributed to the C2 methyl ether versus the free C2 alcohol which could not be ruled out in the present studies.

cm^{-1}; FABHRMS (NBA–NaI) *m/e* 385.1097 (M^+ + Na, $C_{15}H_{22}O_{10}$ requires 385.1111).

3,4,6-Tri-*O*-acetyl-2-*O*-methyl-β-L-gulopyranose (9). A solution of **8** (0.29 g, 0.80 mmol) in THF (3 mL) was treated with $BnNH_2$ (0.22 mL, 2.0 mmol) at 25 °C. The reaction mixture was stirred for 6 h and concentrated in vacuo. Chromatography (SiO_2, 3 × 15 cm, 66% EtOAc–benzene) afforded **9** (0.15 g, 0.26 g theoretical, 59%) as a colorless syrup: R_f 0.4 (SiO_2, 66% EtOAc–benzene); $[\alpha]^{25}_D$ +12.2 (*c* 0.8, CH_3OH); ^1H NMR ($CDCl_3$, 400 MHz) δ 5.45 (1H, dd, *J* = 3.6, 3.6 Hz), 5.01 (1H, d, *J* = 7.9 Hz), 4.98 (1H, dd, *J* = 0.9, 3.6 Hz), 4.15–4.23 (2H, m), 4.09 (1H, dd, *J* = 4.0, 6.4 Hz), 3.85 (1H, br s), 3.46 (3H, s), 3.31 (1H, dd, *J* = 3.6, 7.9 Hz), 2.15 (3H, s), 2.14 (3H, s), 2.08 (3H, s); ^{13}C NMR ($CDCl_3$, 100 MHz) δ 170.6, 169.4, 169.1, 94.1, 77.7, 70.5, 68.0, 66.6, 62.3, 58.5, 20.8, 20.73, 20.70; IR (neat) ν_{max} 3435, 2939, 1754, 1746, 1732, 1372, 1234, 1165, 1129, 1047 cm^{-1}; FABHRMS (NBA–NaI) *m/e* 343.0093 (M^+ + Na, $C_{13}H_{20}O_9$ requires 343.1005).

3,4,6-Tri-*O*-acetyl-2-*O*-methyl-β-L-gulopyranosyl Diphenyl Phosphate (10). A solution of *n*-BuLi (2.5 M in hexane, 88 μL, 0.22 mmol) was added to a stirred solution of **9** (56.8 mg, 0.18 mmol) in dry THF (0.6 mL) at −78 °C under Ar. The resulting solution was stirred for 15 min at −78 °C before the addition of diphenyl chlorophosphate (45.5 μL, 0.22 mmol). After the mixture was stirred for 15 min at −78 °C, saturated aqueous $NaHCO_3$ (1.2 mL) was added to the reaction mixture. The resulting mixture was extracted with EtOAc (2 × 2 mL). The organic layer was washed with H_2O (2 mL) and saturated aqueous NaCl (2 mL), dried (Na_2SO_4), and concentrated in vacuo. Chromatography (SiO_2, 1 × 13 cm, 20% EtOAc–hexane in the presence of 2% Et_3N, then 33% EtOAc–hexane) provided **10** (34.6 mg, 72.9 mg theoretical, 48%; 67% based on recovered **9**) as a colorless syrup and 16.4 mg (28%) of recovered **9**. For **10**: R_f 0.5 (SiO_2, 50% EtOAc–hexane); $[\alpha]^{25}_D$ −15 (*c* 0.5, $CHCl_3$); ^1H NMR ($CDCl_3$, 400 MHz) δ 7.17–7.38 (10H, m), 5.61 (1H, dd, *J* = 7.8, 7.8 Hz), 5.45 (1H, ddd, *J* = 1.2, 3.8, 3.8 Hz), 4.98 (1H, dd, *J* = 1.5, 3.8 Hz), 4.28 (1H, ddd, *J* = 1.5, 5.8, 7.1 Hz), 4.13 (1H, dd, *J* = 5.8, 11.4 Hz), 4.03 (1H, dd, *J* = 7.1, 11.4 Hz), 3.43 (1H, dd, *J* = 3.8, 7.8 Hz), 3.27 (3H, s), 2.15 (3H, s), 2.13 (3H, s), 2.00 (3H, s); ^{13}C NMR ($CDCl_3$, 100 MHz) δ 170.4, 169.3, 169.0, 150.41 (d, *J* = 7 Hz), 150.38 (d, *J* = 7 Hz), 129.7, 129.6, 125.5, 120.4, (d, *J* = 4 Hz), 120.2 (d, *J* = 5 Hz), 97.3 (d, *J* = 5 Hz), 76.3 (d, *J* = 9 Hz), 71.4, 67.5, 66.5, 61.5, 58.4, 20.8, 20.71, 20.66; IR (neat) ν_{max} 2926, 1750, 1489, 1371, 1295, 1220, 1189, 1162, 1066, 961 cm^{-1}; FABHRMS (NBA-NaI) *m/e* 575.1316 (M^+ + Na, $C_{25}H_{29}O_{12}P$ requires 575.1294).

***erythro*-N^{α}-(Benzyloxy)carbonyl-N^{im}-(triphenylmethyl)-β-(3,4,6-tri-*O*-acetyl-2-*O*-methyl-α-L-gulopyranosyl)-L-histidine Methyl Ester (12).** A solution of **10** (13.5 mg, 24.4 μmol) and **11**[30] (9.1 mg, 16.3 μmol) in CH_2Cl_2–Et_2O (1:2, 120–240 μL) was treated with TMSOTf (9.8 μL, 48.9 μmol) at −16 °C under N_2, and the mixture was stirred for 30 min. Saturated aqueous $NaHCO_3$ (0.5 mL) was added to the reaction mixture at −16 °C, and the mixture was extracted with EtOAc (1.0 mL). The organic layer was washed with saturated aqueous NaCl (0.5 mL), dried (Na_2SO_4), and concentrated in vacuo. Chromatography (SiO_2, 1 × 11 cm, 1–2% CH_3OH–CH_2Cl_2 gradient elution and SiO_2, 1 × 6 cm, 33–50% EtOAc–hexane gradient elution) afforded **12** (9.2 mg, 14.1 mg theoretical, 65%, typically 64–72%) as a colorless syrup: R_f 0.5 (SiO_2, 66% EtOAc–hexane); $[\alpha]^{25}_D$ −44 (*c* 1.0, CH_3OH); ^1H NMR ($CDCl_3$, 400 MHz) δ 7.40 (1H, d, *J* = 1.1 Hz), 7.28–7.37 (14H, m), 7.06–7.13 (6H, m), 6.79 (1H, d, *J* = 1.1 Hz), 6.73 (1H, d, *J* = 8.6 Hz), 5.27 (1H, dd, *J* = 3.7, 3.8 Hz), 5.13 (1H, d, *J* = 12.3 Hz), 5.03–5.11 (3H, m), 4.93 (1H, dd, *J* = 1.0, 3.7 Hz), 4.87 (1H, dd, *J* = 4.3, 8.6 Hz), 4.30 (1H, ddd, *J* = 1.0, 6.4, 6.8 Hz), 3.90 (1H, dd, *J* = 6.8, 11.2 Hz), 3.66 (1H, dd, *J* = 6.4, 11.2 Hz), 3.60 (3H, s), 3.51 (1H, dd, *J* = 3.8, 3.8 Hz), 3.32 (3H, s), 2.11 (3H, s), 1.87 (3H, s), 1.86 (3H, s); ^{13}C NMR ($CDCl_3$, 100 MHz) δ 170.2, 169.8, 169.7, 169.3, 156.1, 141.0, 140.9, 136.5, 129.6, 128.7, 128.42, 128.38, 127.93, 127.87, 120.5, 97.3, 77.2, 74.0, 73.8, 67.9, 66.7, 64.8, 64.3, 61.6, 57.8, 57.6, 52.2, 20.72, 20.67, 20.6; IR (neat) ν_{max} 3342, 2956, 2927, 1747, 1372, 1223, 1052, cm^{-1}; FABHRMS (NBA) *m/e* 864.3326 (M^+ + H, $C_{47}H_{49}N_3O_{13}$ requires 864.3345). Table 4 summarizes typical results in the optimization of this reaction.

***erythro*-N^{im}-(Triphenylmethyl)-β-(3,4,6-tri-*O*-acetyl-2-*O*-methyl-α-L-gulopyranosyl)-L-histidine Methyl Ester (13).** A solution of **12** (34 mg, 38.2 μmol) in CH_3OH (2 mL) was hydrogenated over 10% Pd–C (17 mg) under an atmosphere of H_2 (1 atm) at 25 °C for 40 min. The reaction mixture was filtered through a Celite pad and washed with 1% Et_3N–CH_3OH (20 mL) and concentrated in vacuo. Chromatography (SiO_2, 0.6 × 8 cm, 3.7% CH_3OH–CH_2Cl_2 in the presence of 0.4% Et_3N) provided **13** (21.6 mg, 27.9 mg theoretical, 77%) as a colorless syrup: R_f 0.4 (SiO_2, 10% CH_3OH–CH_2Cl_2); $[\alpha]^{25}_D$ −52 (*c* 0.8, CH_3OH); ^1H NMR ($CDCl_3$, 400 MHz) δ 7.39 (1H, d, *J* = 1.4 Hz), 7.31–7.36 (9H, m), 7.10–7.16 (6H, m), 6.86 (1H, d, *J* = 1.4 Hz), 5.28 (1H, dd, *J* = 3.5, 3.8 Hz), 5.13 (1H, d, *J* = 3.8 Hz), 4.97 (1H, d, *J* = 5.2 Hz), 4.89 (1H, dd, *J* = 1.2, 3.5 Hz), 4.30 (1H, ddd, *J* = 1.2, 6.6, 6.6 Hz), 3.98 (1H, dd, *J* = 6.6, 11.2 Hz), 3.96 (1H, d, *J* = 5.2 Hz), 3.76 (1H, dd, *J* = 6.6, 11.2 Hz), 3.73 (3H, s), 3.49 (1H, dd, *J* = 3.8, 3.8 Hz), 3.35 (3H, s), 2.12 (3H, s), 1.91 (3H, s), 1.73 (3H, s), 1.67 (2H, br s); ^{13}C NMR ($CDCl_3$, 100 MHz) δ 172.7, 170.3, 169.5, 169.4, 142.3, 138.9, 129.7, 128.2, 128.1, 120.3, 96.3, 77.3, 75.3, 73.8, 68.3, 65.0, 64.1, 61.7, 58.0, 57.5, 51.8, 20.8, 20.7 (2C); IR (neat) ν_{max} 3379, 2952, 1746, 1493, 1446, 1372, 1225, 1099, 1047 cm^{-1}; FABHRMS (NBA–CsI) *m/e* 862.1984 (M^+ + Cs, $C_{39}H_{43}N_3O_{11}$ requires 862.1952).

***erythro*-N^{α}-((*tert*-Butyloxy)carbonyl)-N^{im}-(triphenylmethyl)-β-(3,4,6-tri-*O*-acetyl-2-*O*-methyl-α-L-gulopyranosyl)-L-histidine Methyl Ester (14).** A solution of **13** (24.0 mg, 32.9 μmol) and $NaHCO_3$ (16.6 mg, 197 μmol) in THF–H_2O (3:1, 2.0 mL) was treated with di-*tert*-butyl dicarbonate (22.7 μL, 98.7 μmol) at 25 °C, and the mixture was allowed to stir for 3 h. EtOAc (5 mL) was added to the reaction mixture, and the organic layer was washed with H_2O (2 mL) and saturated aqueous NaCl (2 mL), dried (Na_2SO_4), and concentrated in vacuo. Chromatography (SiO_2, 0.6 × 7 cm, 50% EtOAc–hexane) gave **14** (25.8 mg, 27.3 mg theoretical, 94%) as a white amorphous powder: R_f 0.6 (SiO_2, 66% EtOAc-hexane); $[\alpha]^{25}_D$ −46 (*c* 1.0, CH_3OH); ^1H NMR ($CDCl_3$, 400 MHz) δ 7.41 (1H, d, *J* = 0.9 Hz), 7.31–7.36 (9H, m), 7.08–7.14 (6H, m), 6.79 (1H, d, *J* = 0.9 Hz), 6.31 (1H, d, *J* = 8.7 Hz), 5.29 (1H, dd, *J* = 3.7, 3.8 Hz), 5.09 (1H, d, *J* = 3.8 Hz), 5.03 (1H, d, *J* = 4.3 Hz), 4.93 (1H, dd, *J* = 1.2, 3.7 Hz), 4.78 (1H, dd, *J* = 4.3, 8.7 Hz), 4.30 (1H, ddd, *J* = 1.2, 6.6, 6.6 Hz), 3.92 (1H, dd, *J* = 6.6, 11.2 Hz), 3.68 (1H, dd, *J* = 6.6, 11.2 Hz), 3.59 (3H, s), 3.53 (1H, dd, *J* = 3.8, 3.8 Hz), 3.38 (3H, s), 2.11 (3H, s), 1.96 (3H, s), 1.86 (3H, s), 1.43 (9H, s); ^{13}C NMR ($CDCl_3$, 100 MHz) δ 170.5, 170.2, 169.9, 169.4, 155.6, 142.2, 139.0, 138.4, 129.7, 128.2, 128.1, 119.8, 96.6, 79.4, 75.4, 75.0, 74.0, 68.2, 65.1, 64.2, 61.7, 57.5, 57.1, 51.9, 28.4, 20.7 (2C), 20.6; IR ($CHCl_3$) ν_{max} 2956, 2930, 1750, 1717, 1369, 1223, 1167, 1053 cm^{-1}; FABHRMS (NBA–CsI) *m/e* 962.2508 (M^+ + Cs, $C_{44}H_{51}N_3O_{13}$ requires 962.2474).

***erythro*-N^{α}-((*tert*-Butyloxy)carbonyl)-N^{im}-(triphenylmethyl)-β-(2-*O*-methyl-α-L-gulopyranosyl)-L-histidine (15).** A solution of **14** (11.7 mg, 14.1 μmol) in CH_3OH (1.5 mL) was treated with aqueous 0.1 N LiOH (0.85 mL, 85 μmol) at 4 °C, and the mixture was stirred for 2.5 h at 4 °C. Aqueous HCl (10%) was added to the reaction mixture for neutralization (pH = 7), and the solvents were removed by evaporation under a N_2 stream. Chromatography (C-18, 0.5 × 3 cm, 0–100% CH_3OH–H_2O gradient elution followed by SiO_2, 0.5 × 6 cm, 10–17% CH_3OH–CH_2Cl_2 gradient elution) provided **15** (6.0 mg, 9.7 mg theoretical, 62%) as a white amorphous solid: R_f 0.3 (SiO_2, 17% CH_3OH–CH_2Cl_2); $[\alpha]^{25}_D$ −12 (*c* 0.45, CH_3OH); ^1H NMR (CD_3OD, 400 MHz) δ 7.51 (1H, s), 7.33–7.42 (9H, m), 7.11–7.19 (6H, m), 7.04 (1H, s), 5.18 (1H, s), 4.94 (1H, s), 4.30–4.65 (2H, m), 3.53–4.08 (5H, m), 3.45 (3H, br s), 1.38 (9H, s); ^{13}C NMR (CD_3OD, 100 MHz) δ 175.4, 157.4, 143.4, 140.0, 138.7, 131.0, 129.5, 129.4, 122.3, 99.8, 80.6, 77.3, 76.9, 75.5, 71.0, 69.6, 67.8, 62.0, 59.4, 57.1, 28.8; IR (KBr) ν_{max} 3423, 2932, 1702, 1618, 1163, 1096, 1049 cm^{-1}; FABHRMS (NBA–CsI) *m/e* 822.2031 (M^+ + Cs, $C_{37}H_{43}N_3O_{10}$ requires 822.2003).

Table 4. *O*-Glycosidation of **11** with **10**

scale, mg of **10**	equiv of **11**	temp (°C)	reactn time (min)	yield (%)
10.0	1.0	0	15	18
13.5	0.67	−16	30	65
34.6	0.67	−16	30	64
51.1	0.50	−30 to −20	60	72
48.1	0.67	−30 to −20	60	64

N^{α}-((*tert*-Butyloxy)carbonyl)-1-[[4(*S*)-(((1(*S*)-(((2-(4′-(((3-(dimethylsulfonio)-1-propyl)amino)carbonyl)-2′,4-bithiazol-2-yl)-1-ethyl)amino)carbonyl)-2(*R*)-hydroxy-1-propyl)amino)carbonyl)-3(*S*)-hydroxy-2(*R*)-pentyl]amino]-N^{im}-(triphenylmethyl)-*erythro*-β-(2-*O*-methyl-α-L-gulopyranosyl)-L-histidine (17). DMF (100 μL) was added to a mixture of **15** (4.9 mg, 7.1 μmol), tetrapeptide S (**16**,[30] 4.9 mg, 7.8 μmol), DCC (4.8 mg, 23.3 μmol), HOBt (1.7 mg, 12.6 μmol), and $NaHCO_3$ (2.1 mg, 25.0 mmol) at 0 °C under N_2, and the reaction mixture was stirred for 22 h at 25 °C under N_2. After concentration in vacuo, the reaction product was triturated with CH_2Cl_2 (4 × 2 mL). Chromatography of the residue (C-18, 0.5 × 4.5 cm, 0−80% CH_3OH-H_2O gradient elutioin) afforded **17** (6.8 mg, 8.9 mg theoretical, 76%) as a white amorphous solid: R_f 0.5 (SiO_2, 10:9:1 CH_3OH−10% aqueous NH_4OAc−10% aqueous NH_4OH); $[\alpha]^{23}_D$ −2.9 (*c* 0.24, CH_3OH); ^1H NMR (CD_3OD, 400 MHz) δ 8.19 (1H, s), 8.10 (1H, s), 7.42 (1H, s), 7.32−7.40 (9H, m), 7.09−7.15 (6H, m), 7.02 (1H, s), 5.06 (1H, d, *J* = 3.0 Hz), 4.82 (1H, d, *J* = 5.3 Hz), 4.45 (1H, d, *J* = 5.3 Hz), 4.31 (1H, d, *J* = 4.2 Hz), 4.10 (1H, dq, *J* = 4.2, 6.4 Hz), 4.03−4.07 (1H, m), 3.93−4.00 (1H, m), 3.77−3.90 (2H, m), 3.73 (1H, dd, *J* = 6.0, 6.8 Hz), 3.65 (2H, t, *J* = 6.8 Hz), 3.56−3.62 (3H, m), 3.45 (3H, s), 3.34−3.45 (4H, m), 3.26 (2H, t, *J* = 6.8 Hz), 2.93 (6H, s), 2.57 (1H, dq, *J* = 6.8, 6.8 Hz), 2.14 (2H, tt, *J* = 6.6, 6.8 Hz), 1.41 (9H, s), 1.13 (3H, d, *J* = 6.4 Hz), 1.10 (3H, d, *J* = 6.9 Hz), 1.07 (3H, d, *J* = 6.8 Hz); IR (KBr) ν_{max} 3422, 2975, 2931, 1655, 1560, 1544, 1162, 1128, 1097, 1052 cm^{-1}; FABHRMS (NBA) *m/e* 1258.4999 (M^+, $C_{61}H_{80}N_9O_{14}S$ requires 1258.4987).

1-[[4(*S*)-(((1(*S*)-(((2-(4′-(((3-(dimethylsulfonio)-1-propyl)amino)carbonyl)-2′,4-bithiazol-2-yl)-1-ethyl)amino)carbonyl)-2(*R*)-hydroxy-1-propyl)amino)carbonyl)-3(*S*)-hydroxy-2(*R*)-pentyl]amino]-N^{im}-(triphenylmethyl)-*erythro*-β-(2‴-*O*-methyl-α-L-gulopyranosyl)-L-histidine (18). Compound **17** (4.9 mg, 3.7 μmol) was treated with 1 N HCl in 90% aqueous HOAc (150 μL) at 25 °C, and the mixture was stirred for 5 min. After concentration in vacuo, the residue was triturated with CH_2Cl_2 (3 × 1 mL) and dried. The residue was dissolved in CH_3OH (0.5 mL), 30% NH_4OH (13 μL) was added, and the mixture was stirred for 2 h at 25 °C before being concentrated in vacuo. Chromatography (C-18, 0.5 × 3 cm, 0−80% CH_3OH-H_2O gradient elution) afforded **18** (2.8 mg, 3.2 mg theoretical, 89%) as a white amorphous powder and 1.5 mg (30%) of recovered **17**. For **18**: R_f 0.2 (SiO_2, 10:9:1 CH_3OH−10% aqueous NH_4OAc−10% aqueous NH_4OH); $[\alpha]^{23}_D$ −10.7 (*c* 0.14, CH_3OH); ^1H NMR (CD_3OD, 400 MHz) δ 8.20 (1H, s), 8.10 (1H, s), 7.45 (1H, s), 7.32−7.39 (9H, m), 7.11−7.18 (6H, m), 7.01 (1H, s), 5.12 (1H, d, *J* = 2.9 Hz), 4.74 (1H, d, *J* = 6.0 Hz), 4.29 (1H, d, *J* = 4.3 Hz), 4.10 (1H, dq, *J* = 4.3, 6.4 Hz), 4.00−4.05 (1H, m), 3.87−3.97 (2H, m), 3.72−3.79 (2H, m), 3.54−3.72 (4H, m), 3.59 (2H, t, *J* = 6.4 Hz), 3.43−3.50 (4H, m), 3.41 (3H, s), 3.27 (2H, t, *J* = 6.4 Hz), 2.93 (6H, s), 2.57 (1H, dq, *J* = 6.8, 6.8 Hz), 2.14 (2H, tt, *J* = 6.6, 7.2 Hz), 1.15 (3H, d, *J* = 6.8 Hz), 1.12 (3H, d, *J* = 6.4 Hz), 1.10 (3H, d, *J* = 5.7 Hz); IR (KBr) ν_{max} 3396, 2931, 1654, 1550, 1448, 1127, 1095, 1045, 988 cm^{-1}; FABMS (NBA) *m/e* 1158 (M^+, $C_{56}H_{72}N_9O_{12}S_3$).

N^{α}-((*tert*-Butyloxy)carbonyl)-N^{β}-[3(*S*)-[4-amino-6-[[[1(*R*)-(((4(*S*)-(((1(*S*)-(((2-(4′-(((3-(dimethylsulfonio)-1-propyl)amino)carbonyl)-2′,4-bithiazol-2-yl)-1-ethyl)amino)carbonyl)-2(*R*)-hydroxy-1-propyl)amino)carbonyl)-3(*S*)-hydroxy-2(*R*)-pentyl)amino)carbonyl)-2(*R*)-(2-*O*-methyl-α-L-gulopyranosyl)-2(*R*)-(1-(triphenylmethyl)imidazol-4-yl)-1-ethyl]amino]carbonyl]-5-methylpyrimidin-2-yl]-1-amino-1-oxo-3-propyl]-(*S*)-β-aminoalanine Amide (20). DMF (20 μL) was added to a mixture of **18** (0.58 mg, 0.50 μmol), **19**[30] (0.26 mg, 0.50 μmol), DCC (0.31 mg, 1.50 μmol), and HOBt (0.10 mg, 0.74 μmol) at 0 °C under Ar, and the mixture was stirred for 24 h at 25 °C. After concentration in vacuo, the residue was triturated with CH_2Cl_2 (2 × 0.5 mL) and dried. Chromatography (C-18, 0.5 × 1 cm, 0−80% CH_3OH-H_2O gradient elution) provided **20** (0.57 mg, 0.78 mg theoretical, 73%) as a white amorphous solid: R_f 0.5 (SiO_2, 10:9:1 CH_3OH−10% aqueous NH_4OAc−10% aqueous NH_4OH); $[\alpha]^{22}_D$ −2.0 (*c* 0.1, CH_3OH); ^1H NMR (CD_3OD, 400 MHz) δ 8.19 (1H, s), 8.09 (1H, s), 7.47 (1H, s), 7.24−7.38 (9H, m), 7.02−7.14 (7H, m), 5.17 (1H, d, *J* = 3.3 Hz), 5.08 (1H, d, *J* = 7.0 Hz), 4.97 (1H, d, *J* = 7.0 Hz), 4.30 (1H, d, *J* = 4.3 Hz), 4.04−4.15 (1H, m), 4.10 (1H, dq, *J* = 4.5, 6.3 Hz), 3.84−4.02 (5H, m), 3.75−3.79 (1H, m), 3.72 (1H, dd, *J* = 5.4, 6.8 Hz), 3.52−3.69 (4H, m), 3.59 (2H, t, *J* = 6.4 Hz), 3.34−3.46 (5H, m), 3.22−3.28 (2H, m), 2.93 (6H, s), 2.67−2.86 (2H, m), 2.48−2.66 (2H, m), 2.41 (1H, dd, *J* = 8.6, 14.6 Hz), 2.28 (3H, s), 2.14 (2H, tt, *J* = 6.8, 6.8 Hz), 1.41 (9H, s), 1.04−1.18 (9H, m); IR (KBr) ν_{max} 3382, 2924, 1654, 1552, 1450, 1382, 1099 cm^{-1}; FABMS (NBA) *m/e* 1566 (M^+ + H, $C_{73}H_{97}N_{16}O_{17}S_3$).

N^{β}-[3(*S*)-[4-Amino-6-[[[1(*R*)-(((4(*S*)-(((1(*S*)-(((2-(4′-(((3-(dimethylsulfonio)-1-propyl)amino)carbonyl)-2′,4-bithiazol-2-yl)-1-ethyl)amino)carbonyl)-2(*R*)-hydroxy-1-propyl)amino)carbonyl)-3(*S*)-hydroxy-2(*R*)-pentyl)amino)carbonyl)-2(*R*)-(2-*O*-methyl-α-L-gulopyranosyl)-2(*R*)-(imidazol-4-yl)-1-ethyl]amino]carbonyl]-5-methylpyrimidin-2-yl]-1-amino-1-oxo-3-propyl]-(*S*)-β-aminoalanine Amide (3). Compound **20** (2.0 mg, 1.3 μmol) was treated with 20% $CF_3CO_2H-CH_2Cl_2$ (200 μL) at 4 °C under Ar, and the mixture was stirred for 2.5 h at 4 °C. The reaction mixture was concentrated under a N_2 stream, and CH_3OH (0.4 mL) and 30% aqueous NH_4OH (10 μL) were added to the residue. After stirring for 1 h at 25 °C, the mixture was concentrated under a N_2 stream. Chromatography (C-18, 0.5 × 2 cm, 0−40% CH_3OH-H_2O gradient elution) afforded **3** (1.2 mg, 1.6 mg theoretical, 77%) as a white amorphous solid: R_f 0.1 (SiO_2, 10:9:1 CH_3OH−10% aqueous NH_4OAc−10% aqueous NH_4OH); $[\alpha]^{22}_D$ −1.7 (*c* 0.1, CH_3OH); ^1H NMR (CD_3OD, 400 MHz) δ 8.21 (1H, s), 8.11 (1H, s), 7.72 (1H, s), 7.20 (1H, s), 5.17−5.27 (2H, m), 4.99 (1H, d, *J* = 4.0 Hz), 4.28 (1H, d, *J* = 4.2 Hz), 3.81−4.18 (6H, m), 4.11 (1H, dq, *J* = 4.2, 6.2 Hz), 3.36−3.76 (13H, m), 3.27−3.29 (2H, m), 2.93 (6H, s), 2.49−2.86 (4H, m), 2.28−2.37 (1H, m), 2.27 (3H, s), 2.15 (2H, tt, *J* = 6.8, 6.8 Hz), 1.13 (3H, d, *J* = 6.2 Hz), 1.11 (3H, d, *J* = 5.8 Hz), 1.08 (3H, d, *J* = 6.9 Hz); IR (KBr) ν_{max} 3436, 2923, 1672, 1590, 1559, 1384, 1205, 1139 cm^{-1}; FABHRMS (NBA) *m/e* 1223.4714 (M^+, $C_{49}H_{75}N_{16}O_{15}S_3$ requires 1223.4760).

2,3,4,6-Tetra-*O*-acetyl-α-D-mannopyranosyl Diphenyl Phosphate (24). A solution of *n*-BuLi (0.66 mL, 1.65 mmol, 2.5 M in hexane) was added to a stirred solution of 2,3,4,6-tetra-*O*-acetyl-α-D-mannose **23**[37] (0.48 g, 1.38 mmol) in dry THF (5 mL) at −78 °C under N_2. The resulting solution was stirred for 20 min at −78 °C before the addition of diphenyl chlorophosphate (0.34 mL, 1.65 mmol). After stirring for 25 min at −78 °C, saturated aqueous $NaHCO_3$ (5 mL) was added to the reaction mixture. The resulting mixture was poured into a two-phase solution of EtOAc (30 mL) and H_2O (20 mL). The organic layer was washed with H_2O (25 mL) and saturated aqueous NaCl (25 mL), dried (Na_2SO_4), and concentrated in vacuo. Chromatography (SiO_2, 1.5 × 14 cm, 20% EtOAc−hexane in the presence of 1% Et_3N) gave **4** (0.54 g, 0.80 g theoretical, 64%) as a colorless syrup: R_f 0.6 (SiO_2, 5% CH_3OH-CH_2Cl_2); $[\alpha]^{22}_D$ +40 (*c* 0.5, $CHCl_3$); ^1H NMR ($CDCl_3$, 400 MHz) δ 7.34−7.40 (4H, m), 7.19−7.29 (6H, m), 5.87 (1H, dd, *J* = 1.7, 6.7 Hz), 5.29−5.40 (3H, m), 4.19 (1H, dd, *J* = 4.7, 12.4 Hz), 4.08 (1H, ddd, *J* = 2.2, 4.7, 9.4 Hz), 3.93 (1H, dd, *J* = 2.2, 12.4 Hz), 2.16 (3H, s), 2.05 (3H, s), 2.01 (3H, s), 1.99 (3H, s); ^{13}C NMR ($CDCl_3$, 100 MHz) δ 170.5, 169.7, 169.5 (2C), 150.1 (d, *J* = 7 Hz), 150.0 (d, *J* = 7 Hz), 130.0, 129.9, 125.8, 125.7, 120.2 (d, *J* = 5 Hz), 120.0 (d, *J* = 5 Hz), 96.0 (d, *J* = 6 Hz), 70.7, 68.6 (d, *J* = 12 Hz), 68.1, 65.0, 61.6, 20.7, 20.6, 20.5 (2C); IR (neat) ν_{max} 2983, 1755, 1590, 1488, 1372, 1220, 1187, 1165, 959 cm^{-1}; FABHRMS (NBA−CsI) *m/e* 713.0433 (M^+ + Cs, $C_{26}H_{29}O_{13}P$ requires 713.0400).

2,3,4,6-Tetra-*O*-acetyl-α-D-mannopyranosyl Trichloroacetimidate (25). A solution of **23** (0.52 g, 1.5 mmol) and trichloroacetonitrile (1.5 mL, 15 mmol) in CH_2Cl_2 (10 mL) was treated with NaH (45 mg, 60% in oil, 1.1 mmol) under N_2 at 25 °C, and the mixture was stirred for 15 min at 25 °C. The reaction mixture was filtered through glass filter and washed with EtOAc (10 mL). The organic layer was concentrated in vacuo. Chromatography (SiO_2, 2 × 13 cm, 33% EtOAc−hexane) provided **25** (0.52 g, 0.74 g theoretical, 69%) as a colorless syrup: R_f (SiO_2, 50% EtOAc−hexane); $[\alpha]^{21}_D$ +50 (*c* 1.0, $CHCl_3$); ^1H NMR ($CDCl_3$, 400 MHz) δ 8.79 (1H, s), 6.29 (1H, d, *J* = 1.9 Hz), 5.48 (1H, dd, *J* = 1.9, 2.9 Hz), 5.36−5.44 (2H, m), 4.28 (1H, dd, *J* = 4.8, 12.0 Hz), 4.14−4.23 (2H, m), 2.21 (3H, s), 2.09 (3H, s), 2.07 (3H, s), 2.02 (3H, s); ^{13}C NMR ($CDCl_3$, 100 MHz) δ 170.4, 169.7, 169.6, 169.5, 159.5, 94.3, 71.1, 68.6, 67.7, 65.2, 61.9, 20.7, 20.6 (2C), 20.5; IR (neat) ν_{max} 3318, 2987, 1755, 1682, 1372, 1217, 1047, 798 cm^{-1}; FABHRMS (NBA−CsI) *m/e* 623.9224 (M^+ + Cs, $C_{16}H_{20}Cl_3NO_{10}$ requires 623.9207).

***erythro*-N^{α}-((Benzyloxy)carbonyl)-N^{im}-(triphenylmethyl)-β-(2,3,4,6-tetra-*O*-acetyl-α-D-mannopyranosyl)-L-histidine Methyl Ester (26).**

Method A. A solution of **24** (50 mg, 89 μmol) and **11**[30] (24 mg, 41 μmol) in Et_2O–CH_2Cl_2 (2:1, 1.5 mL) was treated with TMSOTf (25 μL, 122 μmol) under N_2 at 0 °C, and the mixture was stirred for 2 h at 0 °C. Saturated aqueous $NaHCO_3$ (1 mL) was added, and the mixture was extracted with EtOAc (2 × 2 mL). The organic layer was washed with H_2O (2 mL) and saturated aqueous NaCl (2 mL), dried (Na_2SO_4), and concentrated in vacuo. Chromatography (SiO_2, 1 × 9 cm, 1% CH_3OH–CH_2Cl_2 followed by SiO_2, 0.6 × 11 cm, 33–66% EtOAc–hexane gradient elution) gave **26** (11.6 mg, 36.4 mg theoretical, 32% without optimization) as a colorless syrup: R_f 0.6 (SiO_2, 10% CH_3OH–CH_2Cl_2); $[\alpha]^{21}_D$ +38 (*c* 0.5, $CHCl_3$); ^1H NMR ($CDCl_3$, 400 MHz) δ 7.41 (1H, d, *J* = 1.1 Hz), 7.28–7.40 (14H, m), 7.03–7.10 (6H, m), 6.82 (1H, d, *J* = 1.1 Hz), 6.68 (1H, d, *J* = 8.8 Hz), 5.34 (1H, dd, *J* = 3.3, 10.0 Hz), 5.27 (1H, dd, *J* = 10.0, 10.0 Hz), 5.173 (1H, d, *J* = 12.2 Hz), 5.170 (1H, dd, *J* = 1.4, 3.3 Hz), 5.12 (1H, d, *J* = 12.2 Hz), 5.02 (1H, d, *J* = 5.2 Hz), 4.92 (1H, dd, *J* = 5.2, 8.8 Hz), 4.82 (1H, d, *J* = 1.4 Hz), 4.29 (1H, dd, *J* = 5.2, 12.4 Hz), 4.06–4.15 (2H, m), 3.63 (3H, s), 2.14 (3H, s), 2.08 (3H, s), 2.05 (3H, s), 1.97 (3H, s); ^{13}C NMR ($CDCl_3$, 100 MHz) δ 170.7, 170.2, 169.9, 169.7, 169.5, 156.5, 141.9, 139.9, 136.5, 135.1, 129.6, 128.4, 128.20, 128.16, 127.9, 95.0, 75.6, 71.0, 69.7, 69.2, 68.8, 67.0, 66.0, 62.3, 58.4, 52.4, 20.9, 20.74, 20.70, 20.65; IR (neat) ν_{max} 3346, 2956, 1749, 1225, 1046 cm^{-1}; FABHRMS (NBA–CsI) *m/e* 1024.2219 (M^+ + Cs, $C_{48}H_{49}N_3O_{14}$ requires 1024.2269).

Method B. A solution of **25** (9.3 mg, 18.9 μmol) and **11**[30] (5.0 mg, 8.9 μmol) in Et_2O–CH_2Cl_2 (2:1, 250 μL) was treated with TMSOTf (5.3 μL, 26.7 μmol) under N_2 at 0 °C, and the mixture was stirred for 45 min at 0 °C. Saturated aqueous $NaHCO_3$ (0.25 mL) was added, and the mixture was extracted with EtOAc (2 mL). The organic layers was washed with H_2O (1 mL) and saturated aqueous NaCl (1 mL), dried (Na_2SO_4), and concentrated in vacuo. Preparative thin-layer chromatography (SiO_2, 5% CH_3OH–CH_2Cl_2) afforded **26** (1.9 mg, 7.9 mg theoretical, 24%).

***erythro*-N^{im}-(Triphenylmethyl)-β-(2,3,4,6-tetra-*O*-acetyl-α-D-mannopyranosyl)-L-histidine Methyl Ester (27).** A solution of **26** (10.6 mg, 11.9 μmol) in CH_3OH (0.5 mL) was hydrogenated over 10% Pd–C (5.4 mg) under an atmosphere of H_2 (1 atm) at 25 °C for 45 min. The reaction mixture was filtered through a Celite pad, washed with 1% Et_3N–CH_3OH (10 mL), and concentrated in vacuo. Chromatography (SiO_2, 0.5 × 3 cm, 3.2% CH_3OH–CH_2Cl_2 in the presence of 0.4% Et_3N) provided **27** (6.4 mg, 9.0 mg theoretical, 71%) as a colorless syrup: R_f 0.5 (SiO_2, 10% CH_3OH–CH_2Cl_2); $[\alpha]^{25}_D$ +53 (*c* 0.5, CH_3OH); ^1H NMR ($CDCl_3$, 400 MHz) δ 7.44 (1H, d, *J* = 1.3 Hz), 7.31–7.37 (9H, m), 7.07–7.13 (6H, m), 6.89 (1H, d, *J* = 1.3 Hz), 5.31 (1H, dd, *J* = 3.2, 10.0 Hz), 5.26 (1H, dd, *J* = 9.6, 10.0 Hz), 5.13 (1H, dd, *J* = 1.8, 3.2 Hz), 4.79 (1H, d, *J* = 1.8 Hz), 4.78 (1H, d, *J* = 7.4 Hz), 4.29 (1H, dd, *J* = 5.1, 12.3 Hz), 4.11 (1H, dd, *J* = 2.2, 12.3 Hz), 4.03 (1H, d, *J* = 7.4 Hz), 3.99 (1H, ddd, *J* = 2.2, 5.1, 9.6 Hz), 3.75 (3H, s), 2.13 (3H, s), 2.09 (3H, s), 2.03 (3H, s), 1.97 (3H, s), 1.61 (2H, br s); ^{13}C NMR ($CDCl_3$, 100 MHz) δ 173.8, 170.7, 169.8, 169.7, 169.6, 142.1, 139.0, 135.5, 129.7, 128.2, 122.0, 94.0, 75.5, 74.5, 69.7, 68.9, 68.8, 66.1, 62.3, 58.2, 52.1, 20.9, 20.74, 20.69, 20.6; IR (neat) ν_{max} 3386, 3059, 2954, 1749, 1445, 1370, 1225, 1131, 1047 cm^{-1}; FABHRMS (NBA–CsI) *m/e* 890.1864 (M^+ + Cs, $C_{40}H_{43}N_3O_{12}$ requires 890.1901).

***erythro*-N^{α}-((*tert*-Butyloxy)carbonyl)-N^{im}-(triphenylmethyl)-β-(2,3,4,6-tetra-*O*-acetyl-α-D-mannopyranosyl)-L-histidine Methyl Ester (28).** A solution of **27** (6.0 mg, 7.9 μmol) and $NaHCO_3$ (4.0 mg, 47.5 μmol) in THF–H_2O (3:1, 0.4 mL) was treated with di-*tert*-butyl dicarbonate (5.5 μL, 28.3 μmol) at 25 °C, and the mixture was stirred for 1.5 h at 25 °C. EtOAc (2 mL) was added to the reaction mixture, and the organic layer was washed with H_2O (1.5 mL) and saturated aqueous NaCl (2 mL), dried (Na_2SO_4), and concentrated in vacuo. Chromatography (SiO_2, 0.5 × 3 cm, 3% CH_3OH–CH_2Cl_2) gave **28** (6.7 mg, 6.8 mg theoretical, 99%) as a white syrup: R_f 0.6 (SiO_2, 10% CH_3OH–CH_2Cl_2); $[\alpha]^{22}_D$ +42 (*c* 0.7, $CHCl_3$); ^1H NMR ($CDCl_3$, 400 MHz) δ 7.42 (1H, d, *J* = 1.2 Hz), 7.31–7.36 (9H, m), 7.05–7.12 (6H, m), 6.81 (1H, br s), 6.36 (1H, d, *J* = 8.8 Hz), 5.32 (1H, dd, *J* = 3.3, 9.9 Hz), 5.27 (1H, dd, *J* = 9.7, 9.9 Hz), 5.16 (1H, br s), 4.98 (1H, d, *J* = 5.3 Hz), 4.80–4.87 (2H, m), 4.32 (1H, dd, *J* = 4.9, 12.3 Hz), 4.08–4.17 (2H, m), 3.63 (3H, s), 2.14 (3H, s), 2.09 (3H, s), 2.04 (3H, s), 1.96 (3H, s), 1.45 (9H, s); ^{13}C NMR ($CDCl_3$, 100 MHz) δ 170.6 (2C), 169.8, 169.7, 169.4, 155.8, 142.0, 139.8, 135.5, 129.7, 128.2, 128.1, 121.5, 95.4, 79.8, 75.5, 71.5, 69.7, 69.0, 68.9, 66.0, 62.3, 57.9, 52.2, 28.3, 20.9, 20.7 (2C), 20.6; IR ($CHCl_3$) ν_{max} 3060, 2978, 1749, 1714, 1369, 1225, 1048 cm^{-1}; FABHRMS (NBA) *m/e* 858.3488 (M^+ + H, $C_{45}H_{51}N_3O_{14}$ requires 858.3449).

***erythro*-N^{α}-((*tert*-Butyloxy)carbonyl)-N^{im}-(triphenylmethyl)-β-(α-D-mannopyranosyl)-L-histidine (29).** A solution of **28** (13.4 mg, 15.6 μmol) in CH_3OH (2 mL) was treated with aqueous 0.1 N LiOH (1.1 mL, 0.11 mmol) at 4 °C, and the mixture was stirred for 3 h at 4 °C. A solution of 10% aqueous HCl was added to the reaction mixture for neutralization (pH = 7), and the mixture was concentrated under a N_2 stream. Chromatography (C-18, 0.5 × 3 cm, 0–100% CH_3OH–H_2O gradient elution followed by SiO_2, 0.5 × 1.5 cm, 10–20% CH_3OH–CH_2Cl_2 gradient elution) provided **29** (7.0 mg, 10.5 mg theoretical, 67%) as a white amorphous solid: R_f 0.1 (SiO_2, 17% CH_3OH–CH_2Cl_2); $[\alpha]^{22}_D$ +42 (*c* 0.7, CH_3OH); ^1H NMR (CD_3OD, 400 MHz) δ 7.42 (1H, s), 7.35–7.40 (9H, m), 7.10–7.15 (6H, m), 7.00 (1H, s), 4.94 (1H, d, *J* = 6.8 Hz), 4.58 (1H, br s), 4.48 (1H, d, *J* = 6.8 Hz), 3.85 (1H, d, *J* = 9.6 Hz), 3.76 (1H, dd, *J* = 3.2, 9.5 Hz), 3.65–3.74 (3H, m), 3.56 (1H, dd, *J* = 9.6, 9.6 Hz), 1.38 (9H, s); ^{13}C NMR (CD_3OD, 100 MHz) δ 176.3, 157.4, 143.6, 140.3, 137.7, 130.9, 129.4, 129.3, 123.6, 98.1, 80.2, 77.0, 74.8, 72.4 (2C), 72.2, 68.8, 62.9, 61.0, 28.8; IR (KBr) ν_{max} 3399, 2929, 1701, 1611, 1492, 1164, 1128, 1053 cm^{-1}; FABHRMS (NBA-CsI) *m/e* 808.1855 (M^+ + Cs, $C_{36}H_{41}N_3O_{10}$ requires 808.1846).

N^{α}-((*tert*-Butyloxy)carbonyl)-1-[[4(*S*)-(((1(*S*)-(((2-(4′-(((3-(dimethylsulfonio)-1-propyl)amino)carbonyl)-2′,4-bithiazol-2-yl)-1-ethyl)-amino)carbonyl)-2(*R*)-hydroxy-1-propyl)amino)carbonyl)-3(*S*)-hydroxy-2(*R*)-pentyl]amino]-N^{im}-(triphenylmethyl)-*erythro*-β-(α-D-mannopyranosyl)-L-histidine (30). DMF (120 μL) was added to a mixture of **29** (6.1 mg, 9.0 μmol), tetrapeptide S (**16**,[30] 7.9 mg, 12.7 μmol), DCC (3.5 mg, 17.0 μmol), and HOBt (1.6 mg, 11.7 μmol) at −10 °C under N_2, and the reaction mixture was stirred for 10 h at 25 °C. After concentration in vacuo, the reaction mixture was triturated with CH_2Cl_2 (3 × 1 mL), and the residue was dried under a N_2 stream. Chromatography (C-18, 0.5 × 4 cm, 0–80% CH_3OH–H_2O gradient elution) afforded **30** (7.2 mg, 11.2 mg theoretical, 64%) as a white amorphous solid: R_f 0.7 (SiO_2, 10:9:1 CH_3OH–10% aqueous NH_4OAc–10% aqueous NH_4OH); $[\alpha]^{21}_D$ +54 (*c* 0.3, CH_3OH); ^1H NMR (CD_3OD, 400 MHz) δ 8.20 (1H, s), 8.12 (1H, s), 7.47 (1H, s), 7.33–7.40 (9H, m), 7.08–7.15 (6H, m), 7.08 (1H, s), 4.80 (1H, d, *J* = 8.8 Hz), 4.55 (1H, d, *J* = 1.2 Hz), 4.47 (1H, d, *J* = 8.8 Hz), 4.33 (1H, d, *J* = 4.4 Hz), 4.11 (1H, dq, *J* = 4.4, 6.3 Hz), 3.96 (1H, dq, *J* = 5.3, 6.8 Hz), 3.82 (1H, d, *J* = 10.6 Hz), 3.53–3.75 (10H, m), 3.38 (2H, dd, *J* = 7.4, 7.7 Hz), 3.27 (2H, t, *J* = 6.8 Hz), 2.93 (6H, s), 2.60 (1H, dq, *J* = 6.7, 6.7 Hz), 2.15 (2H, dddd, *J* = 6.8, 7.4, 7.4, 7.7 Hz), 1.38 (9H, s), 1.17 (3H, d, *J* = 6.8 Hz), 1.11–1.15 (6H, m); IR (KBr) ν_{max} 3406, 2929, 1654, 1546, 1129, 1052 cm^{-1}; FABHRMS (NBA) *m/e* 1244.4876 (M^+ + H, $C_{60}H_{78}N_9O_{14}S_3$ requires 1244.4830).

1-[[4(*S*)-(((1(*S*)-(((2-(4′-(((3-(dimethylsulfonio)-1-propyl)amino)-carbonyl)-2′,4-bithiazol-2-yl)-1-ethyl)amino)carbonyl)-2(*R*)-hydroxy-1-propyl)amino)carbonyl)-3(*S*)-hydroxy-2(*R*)-pentyl]amino]-N^{im}-(triphenylmethyl)-*erythro*-β-(α-D-gulopyranosyl)-L-histidine (31). Compound **30** (6.2 mg, 5.0 μmol) was treated with 1 N HCl in 90% aqueous HOAc (200 μL) at 25 °C, and the mixture was stirred for 5 min. After concentration in vacuo, the residue was triturated with CH_2Cl_2 (3 × 1 mL) and dried. The product was dissolved in CH_3OH (1 mL) and treated with 30% aqueous NH_4OH (10 μL), and the mixture was stirred for 2 h at 25 °C. After concentration under a N_2 stream, chromatography (C-18, 0.5 × 4 cm, 0–90% CH_3OH–H_2O gradient elution) afforded **31** (3.8 mg, 4.6 mg theoretical, 82%) as a white amorphous solid and 1.2 mg (19%) of recovered **30**. For **31**: R_f 0.3 (SiO_2, 10:9:1 CH_3OH–10% aqueous NH_4OAc–10% aqueous NH_4OH); $[\alpha]^{21}_D$ +45 (*c* 0.2, CH_3OH); ^1H NMR (CD_3OD, 400 MHz) δ 8.20 (1H, s), 8.12 (1H, s), 7.52 (1H, d, *J* = 1.3 Hz), 7.30–7.42 (9H, m), 7.11–7.19 (6H, m), 7.08 (1H, d, *J* = 1.3 Hz), 4.71 (1H, d, *J* = 7.8 Hz), 4.53 (1H, d, *J* = 1.2 Hz), 4.29 (1H, d, *J* = 4.6 Hz), 4.10 (1H, dq, *J* = 4.6, 6.4 Hz), 3.95 (1H, dq, *J* = 5.2, 6.8 Hz), 3.82 (1H, d, *J* = 10.5 Hz), 3.54–3.74 (11H, m), 3.37 (2H, dd, *J* = 7.6, 7.6 Hz), 3.27 (2H, t, *J* = 6.5 Hz), 2.93 (6H, s), 2.55 (1H, dq, *J* = 6.8, 6.8 Hz), 2.14 (2H, dddd, *J* = 6.6, 6.8, 7.6, 7.6 Hz), 1.19 (3H, d, *J* = 6.8 Hz), 1.15 (3H, d, *J* = 6.8 Hz), 1.12 (3H, d, *J* = 6.4 Hz); IR (KBr) ν_{max} 3387, 2933, 1654, 1546, 1128, 1092, 1072 cm^{-1}; FABHRMS (NBA) *m/e* 1144.4345 (M^+ + H, $C_{55}H_{70}N_9O_{12}S_3$ requires 1144.4306).

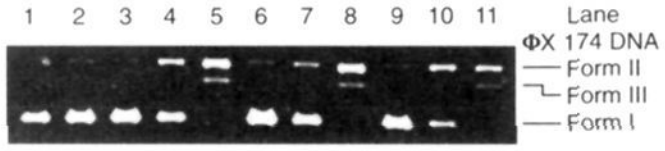

Figure 4. Cleavage of supercoiled ΦX174 DNA by Fe(II)−**3** and related agents. Solutions contained 0.25 μg of supercoiled ΦX174 DNA (1.4×10^{-8} M) in 50 mM Tris-HCl (pH 8.0) containing 10 mM 2-mercaptoethanol. The DNA cleavage reactions were run for 1 h at 25 °C, and electrophoresis was conducted at 50 V for 3 h on a 1% agarose gel containing 0.1 μg/mL ethidium bromide. Lane 1, control ΦX174 DNA, 95% form I (supercoiled), 5% form II (circular); lane 2, 4.0 μM Fe(II) control; lanes 3−5, 0.1, 0.2, and 0.5 μM Fe(II)−**1** (bleomycin A_2); lanes 6−8, 0.5, 1.0, and 2.0 μM Fe(II)−**2** (deglycobleomycin A_2); lanes 9−11, 0.2, 0.5, and 1.0 μM Fe(II)−**3** (demannosylbleomycin A_2). Form I = supercoiled DNA, form II = relaxed DNA (single strand cleavage), form III = linear DNA (double strand cleavage). The gel was immediately visualized on a UV transilluminator and photographed using Polaroid T667 black and white instant film, and the background for the figure has been computer enhanced. Direct fluorescence quantitation was conducted on a Millipore BioImage 60S RFLP system in the presence of ethidium bromide. The results are tabulated in Table 5.

Table 5. Cleavage of Supercoiled ΦX174 DNA by **1**, **2**, and **3**[a]

lane	agent	concentrations (μM)	% form I	% form II	% form III
1	none	0	95	5	0
2	Fe(II)	4	86	14	0
3	bleomycin A_2 (**1**)	0.1	87	11	2
4	bleomycin A_2 (**1**)	0.2	62	32	6
5	bleomycin A_2 (**1**)	0.5	0	73	27
6	deglycobleomycin A_2 (**2**)	0.5	88	12	0
7	deglycobleomycin A_2 (**2**)	1.0	78	22	0
8	deglycobleomycin A_2 (**2**)	2.0	0	75	25
9	demannosylbleomycin A_2 (**3**)	0.2	84	14	2
10	demannosylbleomycin A_2 (**3**)	0.5	41	47	12
11	demannosylbleomycin A_2 (**3**)	1.0	0	66	34

[a] The quantitation of form I, form II, and form III DNA present at each lane of Figure 4 was conducted by direct fluorescence quantitation of the DNA in the presence of ethidium bromide on a Millipore BioImage 60S RFLP system visualized on a UV (312 nm) transilluminator taking into account the relative fluorescence intensities of forms I−III ΦX174 DNA (forms II and III fluorescence intensities are 0.7 times that of Form I).

***N*$^{\alpha}$-((*tert*-Butyloxy)carbonyl)-*N*$^{\beta}$-[3(*S*)-[4-amino-6-[[[1(*R*)-(((4(*S*)-(((1(*S*)-(((2-(4′-(((3-(dimethylsulfonio)-1-propyl)amino)carbonyl)-2′,4-bithiazol-2-yl)-1-ethyl)amino)carbonyl)-2(*R*)-hydroxy-1-propyl)-amino)carbonyl)-3(*S*)-hydroxy-2(*R*)-pentyl)amino)carbonyl)-2(*R*)-(α-D-mannopyranosyl)-2(*R*)-(1-(triphenylmethyl)imidazol-4-yl)-1-ethyl]amino]carbonyl]-5-methylpyrimidin-2-yl]-1-amino-1-oxo-3-propyl]-(*S*)-β-aminoalanine Amide (32).** DMF (120 μL) was added to a mixture of **31** (3.8 mg, 3.3 μmol), **19**[30] (1.8 mg, 3.5 μmol), DCC (1.4 mg, 6.6 μmol), and HOBt (0.6 mg, 4.3 μmol) at 0 °C under N_2, and the mixture was stirred for 10 h at 25 °C. After concentration in vacuo, the residue was triturated with CH_2Cl_2 (3 × 1 mL) and then dried. Chromatography (C-18, 0.5 × 3.7 cm, 0−90% CH_3OH-H_2O gradient elution) provided **32** (4.2 mg, 5.1 mg theoretical, 81%) as a white amorphous solid: R_f 0.7 (SiO_2, 10:9:1 CH_3OH−10% aqueous NH_4OAc−10% aqueous NH_4OH); $[\alpha]^{22}_D$ +39 (*c* 0.13, CH_3OH); ^1H NMR (CD_3OD, 400 MHz) δ 8.20 (1H, s), 8.09 (1H, s), 7.47 (1H, d, *J* = 1.2 Hz), 7.22−7.36 (9H, m), 7.14 (1H, d, *J* = 1.2 Hz), 7.00−7.09 (6H, m), 5.08 (1H, d, *J* = 8.8 Hz), 4.93 (1H, d, *J* = 8.8 Hz), 4.61 (1H, d, *J* = 1.5 Hz), 4.30 (1H, d, *J* = 4.6 Hz), 4.06−4.14 (2H, m), 3.99 (1H, dq, *J* = 4.9, 6.8 Hz), 3.87 (1H, dd, *J* = 5.0, 8.2 Hz), 3.81 (1H, d, *J* = 10.8 Hz), 3.56−3.78 (10H, m), 3.78 (2H, dd, *J* = 7.6, 7.6 Hz), 3.26 (2H, t, *J* = 6.9 Hz), 2.93 (6H, s), 2.66−2.86 (2H, m), 2.46−2.62 (2H, m), 2.36 (1H, dd, *J* = 8.8, 15.0 Hz), 2.25 (3H, s), 2.14 (2H, dddd, *J* = 6.9, 6.9, 7.6, 7.6 Hz), 1.42 (9H, s), 1.19 (3H, d, *J* = 6.8 Hz), 1.16 (3H, d, *J* = 7.0 Hz), 1.11 (3H, d, *J* = 6.4 Hz); IR (KBr) ν_{max} 3396, 2928, 1654, 1546, 1161, 1128 cm^{-1}; FABHRMS (NBA) *m/e* 1522 (M^+ + H, $C_{72}H_{95}N_{16}O_{17}S_3$).

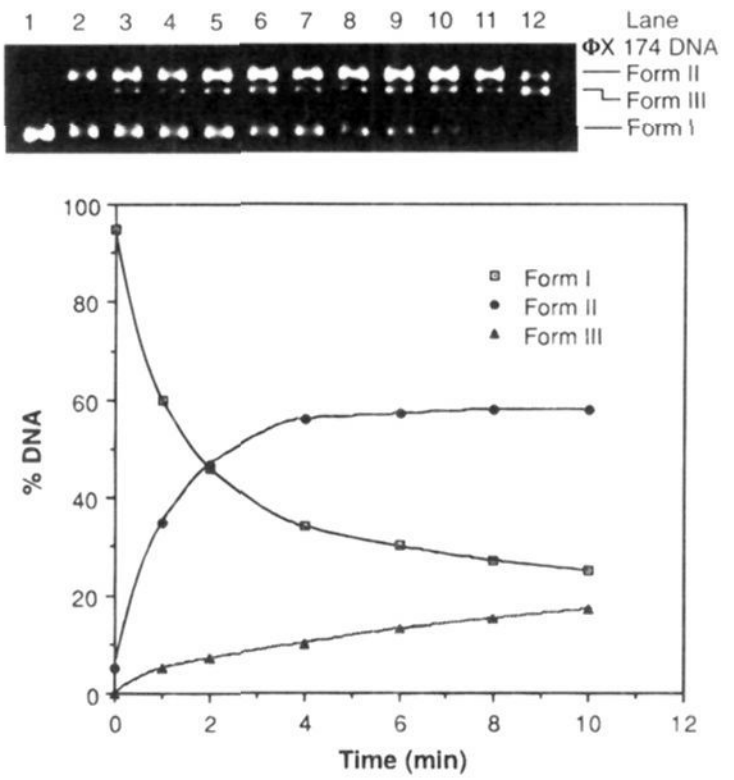

Figure 5. (A, Top) Agarose gel illustraing the kinetics of supercoiled ΦX174 DNA cleavage by Fe(II)−**3** (1 μM). Reaction conditions: solutions contained 0.25 μg of supercoiled ΦX174 DNA (1.4×10^{-8} M) in 50 mM Tris-HCl buffer (pH 8.0) containing 10 mM 2-mercaptoethanol. The DNA cleavage reactions were run at 25 °C, and electrophoresis was conducted at 50 V for 3 h on a 1.0% agarose gel containing 0.1 μg/mL ethidium bromide. Lanes 1−12, extent of the reaction at time = 0, 1, 2, 4, 6, 8, 10, 15, 20, 30, 40, and 60 min. The background for Figure 5 has been computer enhanced. Form I = supercoiled DNA, form II = relaxed DNA (circular, single strand cleavage), form III = linear DNA (double strand cleavage). (B, Bottom) The quantitation of percentage of forms I, II, and III DNA present at each time point. Direct fluorescence quantitation of the DNA in the presence of ethidium bromide was conducted using a Millipore BioImage 60S RFLP system visualized on a UV (312 nm) transilluminator taking into account the relative fluorescence intensities of forms I−III ΦX174 DNA (forms II and III have fluorescence intensities that are 0.7 times that of form I).

***N*$^{\beta}$-[3(*S*)-[4-Amino-6-[[[1(*R*)-(((4(*S*)-(((1(*S*)-(((2-(4′-(((3-(dimethylsulfonio)-1-propyl)amino)carbonyl)-2′,4-bithiazol-2-yl)-1-ethyl)-amino)carbonyl)-2(*R*)-hydroxy-1-propyl)amino)carbonyl)-3(*S*)-hydroxy-2(*R*)-pentyl)amino)carbonyl)-2(*R*)-(α-D-mannopyranosyl)-2(*R*)-(imidazol-4-yl)-1-ethyl]amino]carbonyl]-5-methylpyrimidin-2-yl]-1-amino-1-oxo-3-propyl]-(*S*)-β-aminoalanine Amide (4).** Compound **32** (2.6 mg, 1.7 μmol) was treated with 20% $CF_3CO_2H-CH_2Cl_2$ (200 μL) at 4 °C under N_2, and the mixture was stirred for 2.5 h at 4 °C before the reaction mixture was concentrated under a N_2 stream. The residue was triturated with CH_2Cl_2 (2 × 1 mL), and the residue was dried. The residue was dissolved in CH_3OH (1 mL), 30% aqueous NH_4OH (5 μL) was added, and the mixture was stirred for 1.5 h at 25 °C. After concentration under a N_2 stream, chromatography (C-18, 0.5 × 3 cm, 0−30% CH_3OH-H_2O gradient elution) afforded **4** (1.9 mg, 2.0 mg theoretical, 94%) as a white amorphous solid: R_f 0.2 (SiO_2, 10:9:1 CH_3OH−10% aqueous NH_4OAc−10% aqueous NH_4OH); $[\alpha]^{21}_D$ +41 (*c* 0.09, CH_3OH); ^1H NMR (CD_3OD, 400 MHz) δ 8.21 (1H, s), 8.11 (1H, s), 7.75 (1H, s), 7.29 (1H, s), 5.19 (1H, d, *J* = 7.9 Hz), 4.92 (1H, d, *J* = 7.9 Hz), 4.58 (1H, s), 4.30 (1H, d, *J* = 4.4 Hz), 4.10 (1H, dq, *J* = 4.4, 6.3 Hz), 3.98 (1H, dq, *J* = 5.5, 6.6 Hz), 3.93 (1H, dd, *J* = 5.0, 8.9 Hz), 3.83 (1H, d, *J* = 10.8 Hz), 3.48−3.78 (11H, m), 3.37 (2H, dd, *J* = 7.6, 7.6 Hz), 3.24−3.29 (2H, m, partially obscured by solvent), 2.93 (6H, s), 2.59−2.78 (3H, m), 2.45−2.56 (2H, m), 2.20 (3H, s), 2.15 (2H, dddd, *J* = 6.8, 6.8, 7.6, 7.6 Hz), 1.21 (3H, d, *J* = 6.6 Hz), 1.14 (3H, d, *J* = 6.6 Hz), 1.12 (3H, d, *J* = 6.3 Hz); IR (KBr) ν_{max} 3403, 2930, 1654, 1551, 1201, 1130 cm^{-1}; FABHRMS (NBA) *m/e* 1209.4565 (M^+, $C_{48}H_{73}N_{16}O_{15}S_3$ requires 1209.4603).

General Procedure for the DNA Cleavage Reactions: Supercoiled ΦX174 DNA Relative Efficiency Study. All reactions were run with freshly prepared Fe(II) complexes. The Fe(II) complexes were prepared by combining 1 μL of a H_2O solution of agent at the 10 times specified

Table 6. Relative Efficiency of 5′-End-Labeled w794 DNA Cleavage by **3** and Related Agents[a]

lane	agent	concentration (μM)	IOD	% DNA cleavage	$C \times$ IOD	relative efficiency
1	control DNA	–	18.3	–	–	–
4	bleomycin A_2 (**1**)	0.5	11.8	36	5.9	4.9
5	deglycobleomycin A_2 (**2**)	2.0	14.4	21	28.8	1.0
8	demannosylbleomycin A_2 (**3**)	0.5	12.7	31	6.4	4.5

[a] Quantitation of the consumption of the ^{32}P 5′-end-labeled w794 DNA based on the autoradiograph of the sequencing gel shown in Figure 2 with quantitation conducted using a Millipore BioImage 60S RFLP system, IOD = integrated optical density.

Table 7. Relative Efficiency of 5′-End-Labeled w794 DNA Cleavage by **4** and Related Agents[a]

lane	agent	concentration (μM)	IOD	% DNA cleavage	$C \times$ IOD	relative efficiency
1	control DNA	–	19.2	–	–	–
4	bleomycin A_2 (**1**)	0.5	11.8	39	5.9	5.2
5	deglycobleomycin A_2 (**2**)	2.0	15.4	20	30.8	1
8	mannosyldeglycobleomycin A_2 (**4**)	4.0	12.9	33	51.6	0.6
9	mannosyldeglycobleomycin A_2 (**4**)	8.0	6.6	66	52.8	0.6

[a] Quantitation of the consumption of the ^{32}P 5′-end-labeled w794 DNA based on the autoradiograph of the sequencing gel shown in Figure 3 with quantitation conducted using a Millipore BioImage 60S RFLP system, IOD = integrated optical density.

concentration with 1 μL of a freshly prepared equimolar aqueous $Fe(NH_4)_2(SO_4)_2$ solution followed by vortex mixing and centrifugation. Each of the Fe(II) complex solutions was treated with 7 μL of a buffered DNA solution containing 0.25 μg of a supercoiled ΦX174 RFI DNA (1.4×10^{-8} M) in 50 mM Tris-HCl buffer solution (pH 8). The DNA cleavage reactions were initiated by adding 1 μL of aqueous 10 mM 2-mercaptoethanol. The final concentrations of the agents employed in the study were 2.0 and 4.0 μM Fe(II) control, 0.1, 0.2, 0.5, and 1.0 μM bleomycin A_2 (**1**), 0.2, 0.5, 1.0, and 2.0 μM **3**, 0.2, 0.5, 1.0, 1.5, and 2.0 μM **4**, and 0.5, 1.0, 2.0, and 4.0 μM deglycobleomycin A_2 (**2**). The DNA reaction solution was incubated at 25 °C for 1 h. The reactions were quenched with the addition of 5 μL of loading buffer formed by mixing Keller buffer (0.4 M Tris-HCl, 0.05 M NaOAc, 0.0125 M EDTA, pH 7.9) with glycerol (40%), sodium dodecyl sulfate (0.4%), and bromophenol blue (0.3%). Electrophoresis was conducted on a 1% agarose gel containing 0.1 μg/mL ethidium bromide at 50 V for 3 h, and the gel was immediately visualized on a UV transilluminator and photographed using Polaroid T667 black and white instant film (Figure 4). Direct fluorescence quantitation of DNA in the presence of ethidium bromide was conducted using a Millipore Bio Image 60S RFLP system visualized on a UV (312 nm) transilluminator taking into account the relative fluorescence intensities of forms I–III ΦX174 DNA (form II and III fluorescence intensities are 0.7 times that of form I), and the results are summarized in Table 5.

General Procedure for Quantitation of Double Strand and Single Strand Supercoiled ΦX174 DNA Cleavage. The Fe(II) complexes were formed by mixing 1 μL of 10 μM aqueous solution of **3** or **4** with 1 μL of a freshly prepared 10 μM aqueous $Fe(NH_4)_2(SO_4)_2$. Seven microliters of a buffered DNA solution containing 0.25 μg of supercoiled ΦX174 RFI DNA (1.4×10^{-8} M) in 50 mM Tris-HCl buffer solution (pH 8) were added to each of the complex solutions. The final concentration of **3** and **4** employed in the study was 1 μM. The DNA cleavage reactions were initiated by adding 1 μL of aqueous 10 mM 2-mercaptoethanol to each of the reaction mixtures. The solutions were thoroughly mixed and incubated at 25 °C for 60, 40, 30, 20, 15, 10, 8, 6, 4, 2, and 1 min, respectively. The reactions were quenched with the addition of 5 μL of loading buffer, and electrophoresis was run on a 1% agarose gel containing 0.1 μg/mL ethidium bromide at 50V for 3 h. Direct fluorescence quantitation of the DNA in the presence of ethidium bromide was conducted using a Millipore Bio Image 60S RFLP system taking into account the relative fluorescence intensities of forms I–III ΦX174 DNA (forms II and III fluorescence intensities are 0.7 times that of form I). The ratio of the double to single strand DNA cleavage was calculated with use of the Friefelder–Trumbo equation[39] by assuming a Poisson distribution. Figure 5 illustrates the data for Fe(III)–**3**.

General Procedure for Cleavage of 5′-End-Labeled w794 and w836 DNA: Relative Efficiency and Selectivity. All reactions were run with freshly prepared Fe(III) complexes. The Fe(III) complexes were prepared by combining 1 μL of an aqueous solution of agent at the 10 times specified concentration with 1 μL of a freshly prepared equimolar aqueous $FeCl_3$ solution. Each of the Fe(III) complex solutions were treated with 7 μL of a buffered DNA solution containing the ^{32}P 5′-end-labeled w794 or w836 DNA[41] in 10 mM phosphate buffer (Na_2HPO_4–NaH_2PO_4, pH 7.0) containing 10 mM KCl. The final concentrations of the agents employed in the study were 4.0 and 8.0 μM control Fe(III), 0.2 and 0.5 μM bleomycin A_2 (**1**), 0.2, 0.5, and 1.0 μM **3**, 2.0, 4.0, and 8.0 μM **4**, and 2.0 and 4.0 μM deglycobleomycin A_2 (**2**). The DNA cleavage reactions were initiated by adding 1 μL of 50% aqueous H_2O_2. The DNA reaction solutions were incubated at 37 °C for 30 min. The reactions were quenched with the additions of 2 μL of 50% aqueous glycerol followed by EtOH precipitation and isolation of the DNA. The DNA was resuspended in 6 μL of TE buffer (pH 8.0), and formamide dye (6 μL) was added to the supernatant. Prior to electrophoresis, the samples were warmed at 100 °C for 5 min, placed in an ice bath, and centrifuged, and the supernatant (3 μL) was loaded onto the gel. Sanger dideoxynucleotide sequencing reactions were run as standards adjacent to the agent-treated DNA. Gel electrophoresis was conducted using a denaturing 8% sequencing gel (19:1 acrylamide–*N,N*-methylenebisacrylamide, 8 M urea) at 1100 V for 5.5 h. Formamide dye contained xylene cyanol FF (0.03%), bromophenol blue (0.3%), and aqueous Na_2EDTA (8.7%, 250 mM). Electrophoresis running buffer (TBE) contained Tris base (100 mM), boric acid (100 mM), and Na_2EDTA–H_2O (0.2 mM). Gels were prerun for 30 min with formamide dye prior to loading the samples. Autoradiography of dried gel was carried out at −78 °C using Kodak X-Omat AR film and a Picker spectra intensifying screen. Quantitation of the DNA cleavage reaction was conducted on a Millipore Bio Image 60S RFLP system measuring the remaining uncleaved w794 or w836 DNA. The data for Figures 2 and 3 are summarized in Tables 6 and 7.

Acknowledgment. We gratefully acknowledge the financial support of the National Institutes of Health (CA42056) and the sabbatical leave of ST sponsored by Otsuka Pharmaceutical Co., Ltd.

JA950307B